nature portfolio

Peer Review File

Ocean wave energy harvesting with high energy density and self-powered monitoring system

REVIEWER COMMENTS

Reviewer #1 (Remarks to the Author):

The manuscript submitted to the Journal of Nature Communications proposes a plate-type metamaterial-based energy harvesting structure that converts ocean wave energy into electricity to supply the power required by a wireless monitoring system for the marine Internet of Things. The novel device uses metamaterials to achieve high efficiency and durability in different weather conditions and enables real-time data collection and transmission from the ocean environment. The proposed approach for harvesting electrical energy is novel. The analysis results showed that the designed structure could be applicable in real-world environments.
Major Comments:
1. Authors reviewed the most recent research works related to their work. However, one major concern remains which should be considered before publishing the work. More specifically, authors mostly cited references by reviewing them one after another in a shallow manner without critically discussing them. Thus, what distinguishes the present work from previous studies is still unclear. It is recommended to analyze the most similar works to the authors' manuscript in depth. Plus, the introduction should end with a paragraph explaining the structure of the rest of the paper.
2. Authors have claimed that their proposed design is resistant to harsh weather. However, the results of their analysis did not show such a case. I think the proposed design is more effective in stable conditions than harsh ones. Further, based on the environmental condition explained in Figure 5, I am not yet convinced that the simulated condition explained in Figure 5, e.g., the height and wind speed, does fully simulate harsh weather conditions in the ocean unless the authors prove it otherwise.
3. It was shown in Figure 4.d that the proposed electromagnetic harvesting device only works at a narrow bandwidth of around 2Hz (the local resonance bandgap). Despite its clear effectiveness in supplying power for the monitoring system in this frequency range, how can authors be sure that the excitation frequency of ocean waves is usually around 2Hz?
4. The novelty of the paper is probably less than claimed since similar and improved novel concepts have been already presented in the literature, with which the authors need to compare their novelty; e.g. see:
• Akbari-Farahani, F., & Ebrahimi-Nejad, S. From Defect Mode to Topological Metamaterials: A State-of-the-Art Review of Phononic Crystals & Acoustic Metamaterials for Energy Harvesting. Sensors and Actuators A: Physical, (2023), 114871.
• Krushynska, M. Miniaci, F. Bosia, N. M. Pugno, Coupling local resonance with Bragg band gaps in single-phase mechanical metamaterials. EXTREME MECHANICS LETTERS (2017), 12, 30-36.
• Ravanbod, M., & Ebrahimi-Nejad, S. Perforated auxetic honeycomb booster with reentrant chirality: A new design for high-efficiency piezoelectric energy harvesting. Mechanics of Advanced Materials and Structures, (2023), 1-16.
Minor Comments:
3. Figures presented in the manuscript are designed well. However, a minor issue persists in Figure 3, in particular, Figure 3.c. That is, the manner in which the motion of the electromagnetic energy harvester is shown and explained is confusing.
4. some mistypes were detected as follows:
On line 210, page 12: aa = 0.5g
On line 125, page 8: Fig.1 b (i). There is no subfigure (i) or (ii) in this figure.

Reviewer #2 (Remarks to the Author):

This paper presents the development of a robust, waterproof, floatable metamaterial energy harvesting device. The authors comprehensively discussed the development process, covering design, theoretical aspects, and testing. The work presented is of significance to the energy harvesting field and the paper holds potential for publication in Nature Communications; however, a revision is required and several areas need to be addressed, as outlined below:
Comments:
1. The paper's introduction is well-written, addressing various points. However, the results section

appears to redundantly review aspects previously covered in the introduction. It is suggested to review and revise the first seven lines of the first paragraph in the Results section to avoid redundancy.
2. Adding a paragraph to elaborate on how energy is concentrated in the defective location and the mechanisms behind it would enhance the paper.
3. Clarify how the results in Fig 1b were modeled and how the metamaterial with defects was fabricated.
4. The details of the electromagnetic energy harvesting ball cell in CADs (Figures 1, 2, 3, etc.) lack clarity. Consider providing a better image or a separate figure to discuss the orientation of the ball and its poles against the coils. Include information on coil characteristics, orientation, distance between coils, magnetic ball movement and its magnetic strength. Describe the law governing voltage generation and provide details on sphere diameters.
5. Give detailed information about the charging and discharging series/parallel series of capacitors, including layout, capacitor sizes, and control method of switches S1 and S2.
6. In line 114, specify the unit of the plate size.
7. Discuss the mechanism and role of rolling balls in activating defective inductive balls.
8. Clarify the information presented in Table 1, specifying whether it pertains to the plate or the energy harvesting cell. If the latter, provide details on the ball's dimensions. If the former, explain why the plate is only 6 cm long.
9. Provide a comprehensive description of the graph in Figure 2d, labeling all curves.
10. For Figure 2f, which discusses several geometrical parameters affecting the frequency band, and Figure 2e, claiming optimal results at 1.9 Hz, disclose the specific geometrical values used in modeling for Fig. 2e.
11. Specify the displacement unit in the vertical axis of Figure 2e.
12. It seems that the material selected for the base plate will affect the frequency results and even the amplitude of the vibration in the defective location? Discuss why ABS was chosen for the base plate material and consider exploring other materials and their potential impact on frequency results. Are there any better materials for that? If so, what would be the results if they are used? It is understandable that the authors may not have tested other materials, but if would be great to have at least such a discussion.
13. Add the typical frequency range of ocean waves and clarify the target values for the experiments.
14. Address the potential disparity between testing conducted on a standard shaker, where the plate is positioned on a horizontal shaker base during vibration, and the actual conditions of ocean waves impacting the plate's orientation. The testing scenario on a regular shaker, assuming a fixed orientation, may not precisely replicate the dynamic conditions experienced in the ocean. In reality, ocean waves can cause the plate to shift from a vertical to a horizontal orientation and vice versa. The significance of this discrepancy depends on whether the shaker base is rotatable. If the shaker base is rotatable, this concern may be mitigated. However, additional considerations arise concerning the plate's structure and the location of the energy harvesting cell. In the ocean, waves can approach the plate from any side or even from different sides along the same axis, potentially leading to asymmetry in cell exposure. How have you addressed or justified these factors in your testing methodology?
15. Discuss the implications if the ocean waves cause the plate to flip over. Do you anticipate similar results when the vibration is applied from the other side?
16. Figure 5 discusses the results of the field testing. Provide a comprehensive discussion of the signal transmission system on the plate during field testing with the information such as power consumption, maximum transmission distance, the method of sensor measurement, and the connection of the energy harvester to sensors, etc. Is the system connected through wires? If so, how did you seal it against water?
17. Consider restructuring the paper, and section titles and order to enhance the flow. For example, arrange the theoretical aspect after introducing the design, followed by the description of the device, its fabricated parts, experimental details, and a comprehensive results discussion.
18. Conclusions section is missing.

Reviewer #3 (Remarks to the Author):

A rolling ball water wave energy harvesting design based on the electromagnetic mechanism is introduced in this manuscript and the electrical outputs under various dynamics are shown. Although the design shows some outputs, there are several challenges with the novelty and contribution of the work and the justification for the need for such design:

- The design seems to be simplistic considering a moving magnet above some coils and then multiplying it into multiple units which would provide some small outputs under motions and thus, the novelty in the design is not significant enough.

- The efficient power management given the random nature of water wave motions and multiple units is a big concern and providing a stable output would be a big challenge given the use of complicated electronics would degrade the small output of the system and would not be justified

- The outputs are trivial in the context of water wave energy harvesting and when looking into scaling up the design, more efficient and standard wave generators already exist, so the actual and practical use of such system is unclear rather than powering small electronics which could be powered by a small battery for several years rather than using such complicated mechanism with several units in a relatively large system.

- The effect of random motion and random excitation have not been investigated systematically as it may exist in water waves and is important in realizing whether a stable output would be achieved under such condition or not

The justifications, practicality, and contributions of the proposed system are not sufficient and therefore, it would not be recommended for consideration by the journal.

Responses to the Reviews' Comments

Dear Reviewers,

Thank you for the insightful and helpful comments. We greatly appreciate the comments and suggestions, which have significantly improved the manuscript. Please find our point-by-point responses along with the corresponding revisions/corrections.

Yours Sincerely,

Ze-Qi Lu

on behalf of all the authors

COMMENTS TO THE AUTHOR

Reviewer #1:

The manuscript submitted to the Journal of Nature Communications proposes a plate-type metamaterial-based energy harvesting structure that converts ocean wave energy into electricity to supply the power required by a wireless monitoring system for the marine Internet of Things. The novel device uses metamaterials to achieve high efficiency and durability in different weather conditions and enables real-time data collection and transmission from the ocean environment. The proposed approach for harvesting electrical energy is novel. The analysis results showed that the designed structure could be applicable in real-world environments.

Response: Thank you for your thorough review of our article. Your positive comments are invaluable in enhancing the quality of our article. These changes are highlighted in blue in the revised document. Please find the following point-by-point responses and revisions/corrections.

(1) Authors reviewed the most recent research works related to their work. However, one major concern remains which should be considered before publishing the work. More specifically, authors mostly cited references by reviewing them one after another in a shallow manner without critically discussing them. Thus, what distinguishes the present work from previous studies is still unclear. It is recommended to analyze the

most similar works to the authors' manuscript in depth. Plus, the introduction should end with a paragraph explaining the structure of the rest of the paper.

Response: We have discussed critically the relavent wave energy harvesting devices from the literature in the introduction section and emphasized the novelty of our design. In addition, we added a comparison table to compare our point defect metamaterial energy harvester with existing wave energy harvesting devices in the results section. In addition, the last paragraph of the introduction briefly describes the main focus of this study and explains the structure of the remaining manuscript. The changes to the issues mentioned by the reviewer are listed below.

Changes:

On Page 4

The phenomenon of nonuniformity of the output phase may occur when wave energy is harvested using multiple energy harvesting [37,38,62,63] cells in a device, which can significantly reduce the efficiency of wave energy harvesting. Leveraging the defect state properties of metamaterials enables the concentration of wave energy at the defect location when the wave frequency matches the resonance frequency. This mechanism significantly enhances the efficiency of energy harvesting and ensures a sustainable and stable energy supply for the monitoring system.

On Page 4

The article first describes the design and operational principle of the self-powered energy ocean environment monitoring system in the ocean IoT. Subsequently, it examines the energy concentration characteristics of the point-defective metamaterials used for the energy harvesting function in this monitoring system. Experiments were conducted in the simulated wave environment and the real ocean environment. Finally, the conclusion is presented in the discussion section.

On Page 22

Table 3 compares the structural features and energy output capability of the point defect metamaterial energy harvesting device designed in this study with those of existing wave energy harvesting devices in the literature. Table 3 reveals that the point-defect metamaterial energy harvesting device designed in this study exhibits superior harvesting capability for the kinetic energy of low-frequency waves and offers advantages such as very low internal resistance, high output current, simple structure, and absence of chemical coating compared with the existing harvesting device.

Table 3. Comparison of the structure and energy output capacity for various ocean wave energy harvesting devices.

Parameters	Mutsuda et al. [10]	Kazemi et al. [11]	Zhang et al. [35]	Rodrigues et al. [36]	This work
Type	piezoelectric	piezoelectric	triboelectric	triboelectric	electromagnetic
Structural feature	painted flexible piezoelectric devices	waterproof piezoelectric wave energy harvester	multi-grating triboelectric nanogenerator	rolling-sphere-based triboelectric nanogenerators	Point-defect metamaterial energy harvester
Load resistance (R_L)	1 MΩ	0.7 MΩ	1 MΩ	30 MΩ	6.2 Ω
Output current (I_o)	0.29 mA	14 μA	27.5 μA	2.8 μA	23.23 mA
Output power (P_o)	87.5 mW	0.15 mW	50 μW	230 μW	3.34 mW
Power density [1]	3.5 W/m^2	158 mW/m^2	4.2 mW/m^2	6.02 mW/m^3	99.81 W/m^3

[1] Comparison of power density: piezoelectric sheet and triboelectric sheet are compared in terms of power density per unit area; triboelectric block and electromagnetic block are compared in terms of power density per unit volume.

On Page 29

[10] Mutsuda H, Tanaka Y, Patel R, Doi Y, Moriyama Y, Umino Y. A painting type of flexible piezoelectric device for ocean energy harvesting. Applied Ocean Research, 2017, 68: 182-193.

[11] Rodrigues C, et al. Integrated study of a triboelectric nanogenerator for ocean wave energy harvesting: Performance assessment in realistic sea conditions. Nano Energy, 2021, 84:105190.

On Page 31

[35] Zhang D, Shi J, Si Y, Li T. Multi-grating triboelectric nanogenerator for harvesting low-frequency ocean wave energy. Nano Energy, 2019, 61: 132-140.

[36] Rodrigues C, et al. Integrated study of triboelectric nanogenerator for ocean wave energy harvesting: Performance assessment in realistic sea conditions. Nano Energy, 2021, 84:105190.

On Page 34

[62] Wang, D. Y., Wang, X. X., Jin, M. L., He, P., Zhang, S. Y. Molecular level manipulation of charge density for solid-liquid TENG system by proton irradiation. Nano Energy ,2022, 103:107819

[63] Lv, S. S., Zhang, X., Huang, T., Yu, H., Zhu, M. F. Interconnected array design for enhancing the performance of an enclosed flexible triboelectric nanogenerator. Nano Energy, 2021, 89: 106476

(2) Authors have claimed that their proposed design is resistant to harsh weather. However, the results of their analysis did not show such a case. I think the proposed design is more effective in stable conditions than harsh ones. Further, based on the environmental condition explained in Figure 5, I am not yet convinced that the simulated condition explained in Figure 5, e.g., the height and wind speed, does fully simulate harsh weather conditions in the ocean unless the authors prove it otherwise.

Response: To simulate that the metamaterial wave energy harvesting device can operate effectively under harsh wave environments, we added in Fig. 3 the large excitation experiment on the water tank to simulate the real harsh environment of the metamaterial plate in the ocean. The results confirmed that the device still has a good energy output capacity under harsh environments such as very large waves. Furthermore, In Fig. 5, we added the real-time monitoring data of the ocean environmental health monitoring system in the same ocean area under the night environment. The change to the issues mentioned by the reviewer is below.

Changes:

On Page 13

As illustrated in Figs. 3a and 3b, the experiments simulated wave excitation in both stable and harsh environments, examining the motion states and energy output voltages of the rolling ball within the energy-harvesting metamaterial device under different wave excitation states. In harsh ocean environments such as typhoons, the acceleration of waves is generally greater than 0.5g[64,65], which is related to many factors such as ocean depth, area, and wave period. The acceleration of waves is used as an index to distinguish stable and harsh ocean wave environments. Table 2 shows the conditions used to simulate different types of ocean wave environments. The experiments revealed that when the water tank's acceleration was less than 0.5g, small stable waves were generated. When the acceleration was 0.5g, large stable waves were generated. When the acceleration was larger than 0.5g, the wave becomes huge. When the acceleration was greater than 2g, the waves in the water tank significantly impacted the metamaterial energy harvesting device, occasionally causing the metamaterial plate to flip over. Thus, in this study, the simulated ocean waves under different excitations are classified as stable waves and harsh waves. When the applied acceleration exceeds 2g, the wave impact on the water tank may cause the metamaterial fracture. Consequently, the maximum excitation acceleration is limited to 2g.

Table 2. Conditions of the ocean wave environment simulation experiments

Excitation acceleration[1] [g]	Excitation direction	Metamaterial plate	Silulation of the ocean wave environment
0.1	*x*-direction	no flip	stable
0.5	*x*-direction	no flip	stable
1	*x*-direction	no flip	harsh
1.5	*z*-direction	no flip	harsh
1.5	*x-y* direction	flip	harsh
2	*z*-direction	flip	harsh

[1] In harsh ocean environments such as typhoons, the acceleration of waves is generally greater than 0.5g[64,65], which is related to many factors such as ocean depth, area, and wave period. The acceleration of waves is used as an index to distinguish stable and harsh ocean wave environments.

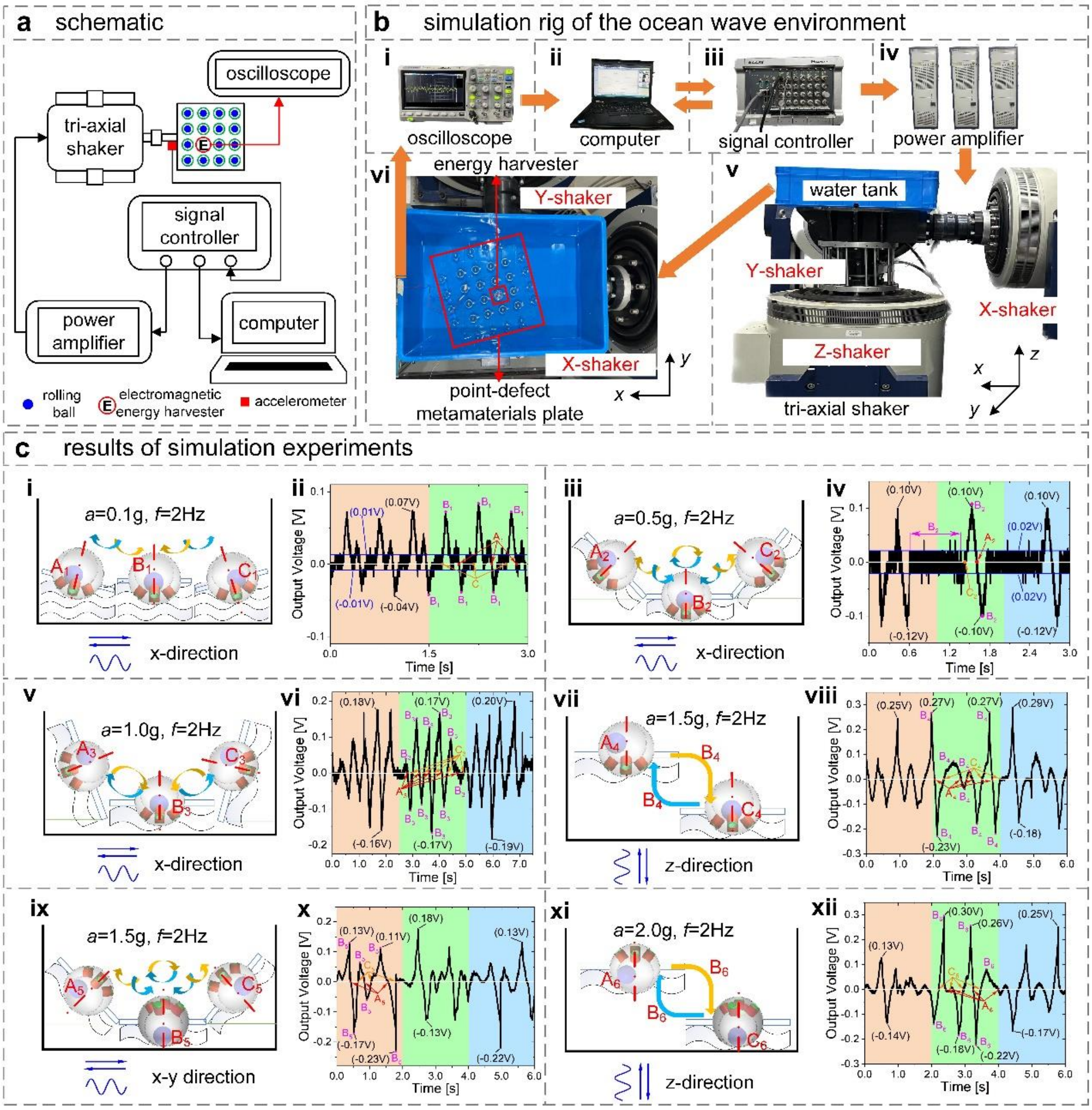

Fig 3. Experiments of the response of a high-density energy-harvesting metamaterial device under various wave size conditions. a. schematic of the experimental rig; b. photographs of the experimental rig: (i) oscilloscope, which shows the energy-harvesting metamaterial plate output voltage; (ii) computer; (iii) signal controller, which generates sinusoidal signals; (iv) power amplifier; (v) triaxial shakers that provide excitation in the *x*-, *y*- and *z*-directions; (vi) flume, which simulates the ocean wave environment; c. motion state analysis and output voltage of a rolling magnetic ball in a metamaterial energy-harvesting device under various wave conditions: (i), (ii): *a*=0.1g, *f*=2Hz, *x*-direction excitation; (iii), (iv): *a* =0.5g, *f* =2Hz, *x* -direction excitation; (v), (vi): *a* =1.0 g, *f* =2Hz, *x*-direction excitation; (vii), (viii): *a* =1.5g, *f* =2Hz, *z*-direction excitation; when the energy harvesting metamaterial plate is in the multi-direction excitation state; (ix), (x): *a* =1.5g, *f* =2Hz, *x* -*y*-direction excitation, when the energy harvesting metamaterial plate is in the multi-direction excitation state; (xi), (xii): *a* = 2.0 g, *f* =2Hz, *z*-direction excitation, when the energy harvesting metamaterial plate is in the overturning state; where (i)-(vi) simulate the motion state and energy output of the rolling ball in the metamaterial energy harvester in a steady wave environment, (vii)–(xii) simulate the motion state and energy output of the rolling ball in the metamaterial energy harvester in a harsh environment.

On Page 14

The motion state and output voltage of the rolling ball in the metamaterial energy harvester under steady wave environments (a<0.5g) and harsh wave environments (a>0.5g) are illustrated in Fig. 3c. The motion analysis of the energy harvester in the point defect metamaterial is mainly discussed around the relative position and velocity of the rolling magnetic ball. The red dotted line in Fig. 3c is the center axis of the rolling magnetic ball energy harvester. This study determines the energy output state of an energy harvester by determining the position and velocity of a rolling magnetic ball relative to the central axis. Fig. 3c(i)-Fig. 3c(vi) simulate the motion state and energy output of the rolling ball in the metamaterial energy harvester in a stable wave environment, and Fig. 3c(vii)-Fig. 3c(xii) simulate the motion state and energy output of the rolling ball in the metamaterial energy harvester in a harsh environment. In the output voltage curve, each color block (orange, green, and blue) represents the complete cycle of motion of a rolling magnetic ball in the energy harvesting device. The output response and motion cycle of the green block are used as examples.

On Page 18

To examine the energy output capability of the metamaterial energy harvesting device and the motion of the rolling magnetic ball in the harsh wave environment, Fig. 3c(vii) simulates the state of the metamaterial plate excited by the "surging wave" from the seafloor, when the triaxial shaker applies vertical excitation to the water tank. When the metamaterial plate is excited by the surface of the ocean in the *z*-direction, the motion of the rolling magnetic ball in the energy harvesting device is monitored. Primarily, the rolling magnetic ball performs a jumping motion away from the surface of the inner shell, i.e., A_4-(yellow arrows)-B_4-(yellow arrows)-C_4, and C_4-(blue arrows)-B_4-(blue arrows)-A_4. Compared with the surface of the ocean, the energy harvesting device of the metamaterial plate is at different heights and moments in time. During the jumping process (B_4), the magnetic ball moves at the maximum speed, when the output voltage is maximum, and the output voltage of the energy harvesting device can be up to 0.27 V, as shown in Fig. 3c(viii). When the rolling magnetic ball occupies positions A_4 and

C_4, it remains relatively static with respect to the inductive coil, resulting in an instantaneous voltage output of 0 V. Simulating the metamaterial energy harvesting device under vertical excitation of the experiment demonstrates that the device has robust energy harvesting ability even under the harsh ocean environment of "surging wave".

In ocean environments, the energy harvesting device can experience asymmetric excitation from multiple directions, resulting in the flipping of the metamaterial energy harvesting device. Fig. 3c(ix) simulates a working condition in which the metamaterial energy harvesting device is subjected to simultaneous *x*-*y* multi-directional excitations in a flipped state. Observing the motion of the energy harvesting device reveals that this device undergoes a rotational motion while moving with the wave, and the rolling sphere also rotates along the inner wall of the ball shell when the rolling magnetic sphere is farther away from the induction coil, i.e., B_5-(yellow arrow)-A_5-(blue arrow)-B_5; B_5-(yellow arrow)-C_5-(blue arrow). In the process of movement, the speed of the rolling magnetic ball relative to the induction coil is maximum in the B_5 state, resulting in the highest instantaneous output voltage of 0.23 V. Conversely, in the A_5 and C_5 states, the speed of the rolling magnetic ball relative to the induction coil is zero, leading to an instantaneous output voltage of 0. In the flip state, as shown in Fig. 3c(x), the output voltage of the metamaterial energy harvesting device decreases. The output voltage of the device in the flip state is 0.23 V. This simulation confirms that the device also exhibits superior energy harvesting capability under asymmetric excitation.

Fig. 3c(xi) simulates the motion state and energy output capability of the energy harvesting metamaterial plate in the overturning state under ultra-large vertical excitation of a = 2.0 g. This simulated environment is an extremely harsh ocean wave environment when the metamaterial plate is also in the up and down state on the ocean wave surface and the rolling magnetic ball in the energy harvester is in a jumping state. Observing the motion of the energy harvesting device reveals that the rolling magnetic ball and the induction coil are in a relatively stationary state at the A_6 and C_6 moments, resulting in an instantaneous output voltage response of 0, as illustrated in Fig. 3c(xii). At moment B_6, the rolling ball in the energy harvesting device is in a jumping state, and the relative velocity between the rolling magnetic ball and the inductive coil is maximum at this instant. Consequently, the output voltage reaches 0.3 V. Given that the excitation of the wave to the energy harvesting device is sufficiently large, the device still maintains a high energy output in the overturning state.

(3) It was shown in Figure 4.d that the proposed electromagnetic harvesting device only works at a narrow bandwidth of around 2Hz (the local resonance bandgap). Despite its clear effectiveness in supplying power for the monitoring system in this frequency range, how can authors be sure that the excitation frequency of ocean waves is usually around 2Hz?

Response: The period of ocean waves is generally 0.5–25 s, which is converted into a frequency of approximately 0.04–2 Hz. The frequency of waves on the coastal ocean surface is approximately 1–2 Hz. To verify this frequency feature and obtain real condition data, we integrated a wave height monitoring function in our ocean environmental condition monitoring system. The time-domain data of the wave height can be Fourier transformed to derive the wave spectrum in the corresponding time. We have added the wave spectrum of the test sea area in Fig. 5. Analysis of the wave spectrum reveals that the wave frequency is distributed across the entire frequency band but is primarily concentrated in the frequency range of 1.4–2.0 Hz, which is also the frequency range of the defective band investigated in this study. Below are the modifications addressing the reviewer's comments.

Changes:

On Page 23

To clarify the target frequency of the metamaterial energy harvesting device for realizing the energy concentration phenomenon, the real-time wave height monitoring function of the energy harvesting device was used to derive the wave height monitoring data. The real-time wave height data at 00:00 and 12:00 were Fourier transformed to obtain the ocean wave spectrum, as illustrated Fig. 5c(i and ii) (the red solid line is the instantaneous wave spectrum at 00:00-00:10 and the blue dashed line is the instantaneous wave spectrum at 12:00-12:10). As shown in Fig. 5b, the ocean wave frequencies are distributed within 0.1–2.1 Hz but are primarily concentrated in the frequency ranges of 0.5–1 Hz and 1.5–1.9 Hz. Therefore, the energy concentration frequency of the metamaterial energy harvesting device locates at those frequency ranges, resulting in better energy harvesting efficiency. Fig. 5c(iii) shows the spectrum of the output power of the high-density energy harvesting metamaterials. It is found that the output power is maximum near the defect band, with the maximum output power of 21.1 mW and 22.8 mW in the two time periods, respectively. Fig. 5d shows the real-time monitoring of ocean information by the ocean environment health monitoring system, which can prove that the self-powered ocean environment monitoring system designed in this work has good practicability.

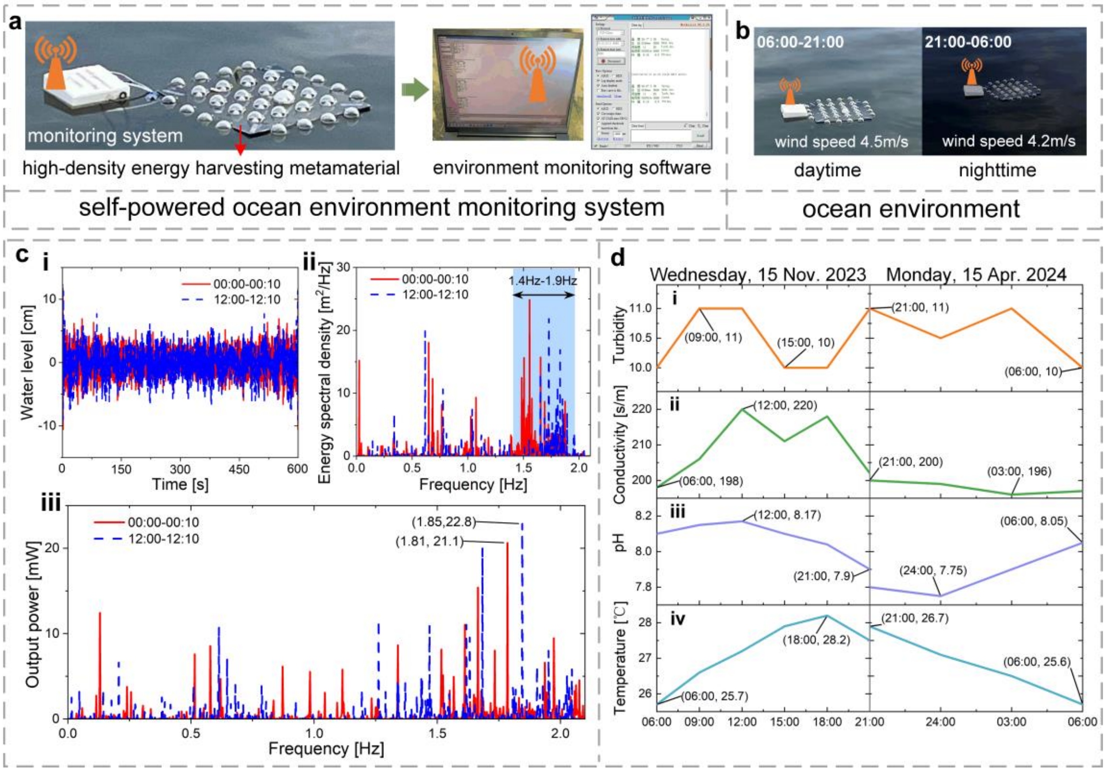

Fig. 5. Self-powered ocean environment monitoring system. a. Self-powered ocean environment monitoring system (High-density energy harvesting metamaterials and environmental monitoring software); b. the real ocean environment: daytime test environment (wind speed of 4.5 m/s) and nighttime test environment (wind speed of 4.2 m/s); c. testing results (red solid line: 00:00-00:10; blue dotted line: 12:00-12:10): (i) spectrum of the wave level; (ii) energy spectral density of the wave; (iii) Output power spectrum of the high-density energy harvesting metamaterial; d. real-time health monitoring results of the ocean environment in one day (24h): (i) turbidity, (ii) conductivity, (iii) pH, and (iv) temperature.

(4) The novelty of the paper is probably less than claimed since similar and improved novel concepts have been already presented in the literature, with which the authors need to compare their novelty; e.g. see:

• Akbari-Farahani, F., & Ebrahimi-Nejad, S. From Defect Mode to Topological Metamaterials: A State-of-the-Art Review of Phononic Crystals & Acoustic Metamaterials for Energy Harvesting. Sensors and Actuators A: Physical, (2023), 114871.

• Krushynska, M. Miniaci, F. Bosia, N. M. Pugno, Coupling local resonance with Bragg band gaps in single-phase mechanical metamaterials. EXTREME MECHANICS LETTERS (2017), 12, 30-36.

• Ravanbod, M., & Ebrahimi-Nejad, S. Perforated auxetic honeycomb booster with reentrant chirality: A new design for high-efficiency piezoelectric energy harvesting. Mechanics of Advanced Materials and Structures, (2023), 1-16.

Response: Thank you for providing the related publications. We compared the point-defect metamaterials in this study with the defective state metamaterials in the literature accordingly. The design develops a novel self-powered sensing node for the sensing network within the ocean IoT system, which for the first time uses the energy concentration effect of point-deficient metamaterials to efficiently harvest wave energy, thereby supplying electrical energy to the sensing nodes. The advantage of this design is that it concentrates energy harvesting at a point on a plane, thereby avoiding the issue of inconsistent AC phase that arises when multiple energy harvesters are placed across the plane. Moreover, the design of the point-defect energy harvester in this study has a defect band adapted to the ocean wave environment which can tune the elastic waves generated during ocean wave fluctuations and concentrate the wave energy at the defect location for efficient energy harvesting. The change to the issues mentioned by the reviewer is below.

Changes:

On Page 3

Ravanbod et al.[59] designed an efficient piezoelectric harvesting device based on the defect state properties of metamaterials; Akbari-Farahani et al. [60] concentrated the sound energy at the defect locations of metamaterials to enhance the acoustic wave energy harvesting; Krushynska et al.[61] investigated the bandgap of metamaterials and designed a single-phase solid metamaterial with a quasi-resonant Bragg bandgap that enables the modulation of elastic waves. The studies above share a common feature: the highest vibrational energy is harvested at the defect band frequencies for both elastic and acoustic vibration energy harvesting. Inspired by these primary discoveries, this study proposes an energy harvesting device for point defect metamaterials that can modulate the elastic waves generated during wave fluctuations and concentrate the in-plane fluctuation wave energy at the defect location for efficient energy harvesting.

On Page 4

This study designs a novel self-powered sensing node for the sensing network in the ocean IoT system, which for the first time applies the energy concentration effect of point-deficient metamaterials for efficient wave energy harvesting to supply electrical energy of the sensing nodes for OIoT systems. This device is waterproof, corrosion-resistant, and unaffected by coatings, allowing for more effective harvesting and conversion of wave energy in extreme weather conditions. Compared with traditional ocean wave energy harvesters, the nonlinear electromagnetic energy harvesting device developed in this study offers the benefits of a simple structure, superior shock resistance, and cost-effectiveness. However, electromagnetic energy harvesting devices generate high-induced currents and low voltages, and the magnitude of the electrical output is affected by the rate of change of the magnetic flux. To address this challenge, this study pioneers the use of the unique defect state characteristics of metamaterials to harvest the scattered vibration energy within the oceam wave environment at the defect location of the metamaterials. The advantage of this design is that it centralizes energy harvesting at a point on a plane, thereby avoiding the issue of inconsistent AC phase that arises when multiple energy harvesters are placed across the plane.

On Page 33

[59] Ravanbod, M., Ebrahimi-Nejad, S. Perforated auxetic honeycomb booster with

reentrant chirality: A new design for high-efficiency piezoelectric energy harvesting. Mechanics of Advanced Materials and Structures, 2023,1-16.

[60] Akbari-Farahani, F., Ebrahimi-Nejad, S. From defect mode to topological metamaterials: A state-of-the-art review of phononic crystals & acoustic metamaterials for energy harvesting. Sensors and Actuators A: Physical, 2024, 114871:365.

[61] Krushynska, A.O., Miniaci, M., Bosia, F., Pugno, N.M. Coupling local resonance with Bragg band gaps in single-phase mechanical metamaterials. Extreme Mechanics Letters, 2017, 30-36 (12).

(5) Figures presented in the manuscript are designed well. However, a minor issue persists in Figure 3, in particular, Figure 3.c. That is, the manner in which the motion of the electromagnetic energy harvester is shown and explained is confusing.

Response: We have added further explanation of the way the rolling ball moves in the energy harvesting device in Fig. 3. The change to the issues mentioned by the reviewer is below.

Changes:

On Page 14

The motion state and output voltage of the rolling ball in the metamaterial energy harvester under steady wave environments ($a<0.5g$) and harsh wave environments ($a>0.5g$) are illustrated in Fig. 3c. The motion analysis of the energy harvester in the point defect metamaterial is mainly discussed around the relative position and velocity of the rolling magnetic ball. The red dotted line in Fig. 3c is the center axis of the rolling magnetic ball energy harvester. This study determines the energy output state of an energy harvester by determining the position and velocity of a rolling magnetic ball relative to the central axis. Fig. 3c(i)-Fig. 3c(vi) simulate the motion state and energy output of the rolling ball in the metamaterial energy harvester in a stable wave environment, and Fig. 3c(vii)-Fig. 3c(xii) simulate the motion state and energy output of the rolling ball in the metamaterial energy harvester in a harsh environment. In the output voltage curve, each color block (orange, green, and blue) represents the complete cycle of motion of a rolling magnetic ball in the energy harvesting device. The output response and motion cycle of the green block are used as examples.

on page 18

To examine the energy output capability of the metamaterial energy harvesting device and the motion of the rolling magnetic ball in the harsh wave environment, Fig. 3c(vii) simulates the state of the metamaterial plate excited by the "surging wave" from the seafloor, when the triaxial shaker applies vertical excitation to the water tank. When the metamaterial plate is excited by the surface of the ocean in the *z*-direction, the motion of the rolling magnetic ball in the energy harvesting device is monitored. Primarily, the rolling magnetic ball performs a jumping motion away from the surface of the inner shell, i.e., A_4-(yellow arrows)-B_4-(yellow arrows)-C_4, and C_4-(blue arrows)-B_4-(blue arrows)-A_4. Compared with the surface of the ocean, the energy harvesting device of the metamaterial plate is at different heights and moments in time. During the jumping process (B_4), the magnetic ball moves at the maximum speed, when the output voltage is maximum, and the output voltage of the energy harvesting device can be up to 0.27 V, as shown in Fig. 3c(viii). When the rolling magnetic ball occupies positions A_4 and C_4, it remains relatively static with respect to the inductive coil, resulting in an instantaneous voltage output of 0 V. Simulating the metamaterial energy harvesting device under vertical excitation of the experiment demonstrates that the device has robust energy harvesting ability even under the harsh ocean environment of "surging wave".

In ocean environments, the energy harvesting device can experience asymmetric excitation from multiple directions, resulting in the flipping of the metamaterial energy harvesting device. Fig. 3c(ix) simulates a working condition in which the metamaterial energy harvesting device is subjected to simultaneous *x*-*y* multi-directional excitations in a flipped state. Observing the motion of the energy harvesting device reveals that this device undergoes a rotational motion while moving with the wave, and the rolling sphere also rotates along the inner wall of the ball shell when the rolling magnetic sphere is farther away from the induction coil, i.e., B_5-(yellow arrow)-A_5-(blue arrow)-B_5; B_5-(yellow arrow)-C_5-(blue arrow). In the process of movement, the speed of the rolling magnetic ball relative to the induction coil is maximum in the B_5 state, resulting in the highest instantaneous output voltage of 0.23 V. Conversely, in the A_5 and C_5 states, the speed of the rolling magnetic ball relative to the induction coil is zero, leading to an instantaneous output voltage of 0. In the flip state, as shown in Fig. 3c(x), the output voltage of the metamaterial energy harvesting device decreases. The output voltage of the device in the flip state is 0.23 V. This simulation confirms that the device also exhibits superior energy harvesting capability under asymmetric excitation.

Fig. 3c(xi) simulates the motion state and energy output capability of the energy harvesting metamaterial plate in the overturning state under ultra-large vertical excitation of a = 2.0 g. This simulated environment is an extremely harsh ocean wave environment when the metamaterial plate is also in the up and down state on the ocean wave surface and the rolling magnetic ball in the energy harvester is in a jumping state. Observing the motion of the energy harvesting device reveals that the rolling magnetic ball and the induction coil are in a relatively stationary state at the A_6 and C_6 moments, resulting in an instantaneous output voltage response of 0, as illustrated in Fig. 3c(xii). At moment B_6, the rolling ball in the energy harvesting device is in a jumping state, and the relative velocity between the rolling magnetic ball and the inductive coil is maximum at this instant. Consequently, the output voltage reaches 0.3 V. Given that the excitation of the wave to the energy harvesting device is sufficiently large, the device still maintains a high energy output in the overturning state.

(6) some mistypes were detected as follows:

On line 125, page 8: Fig.1 b (i). There is no subfigure (i) or (ii) in this figure.

On line 210, page 12: aa = 0.5g

Response: We have revised these typos. Thank you. The change to the issues mentioned by the reviewer is below.

Changes:

On Page 7

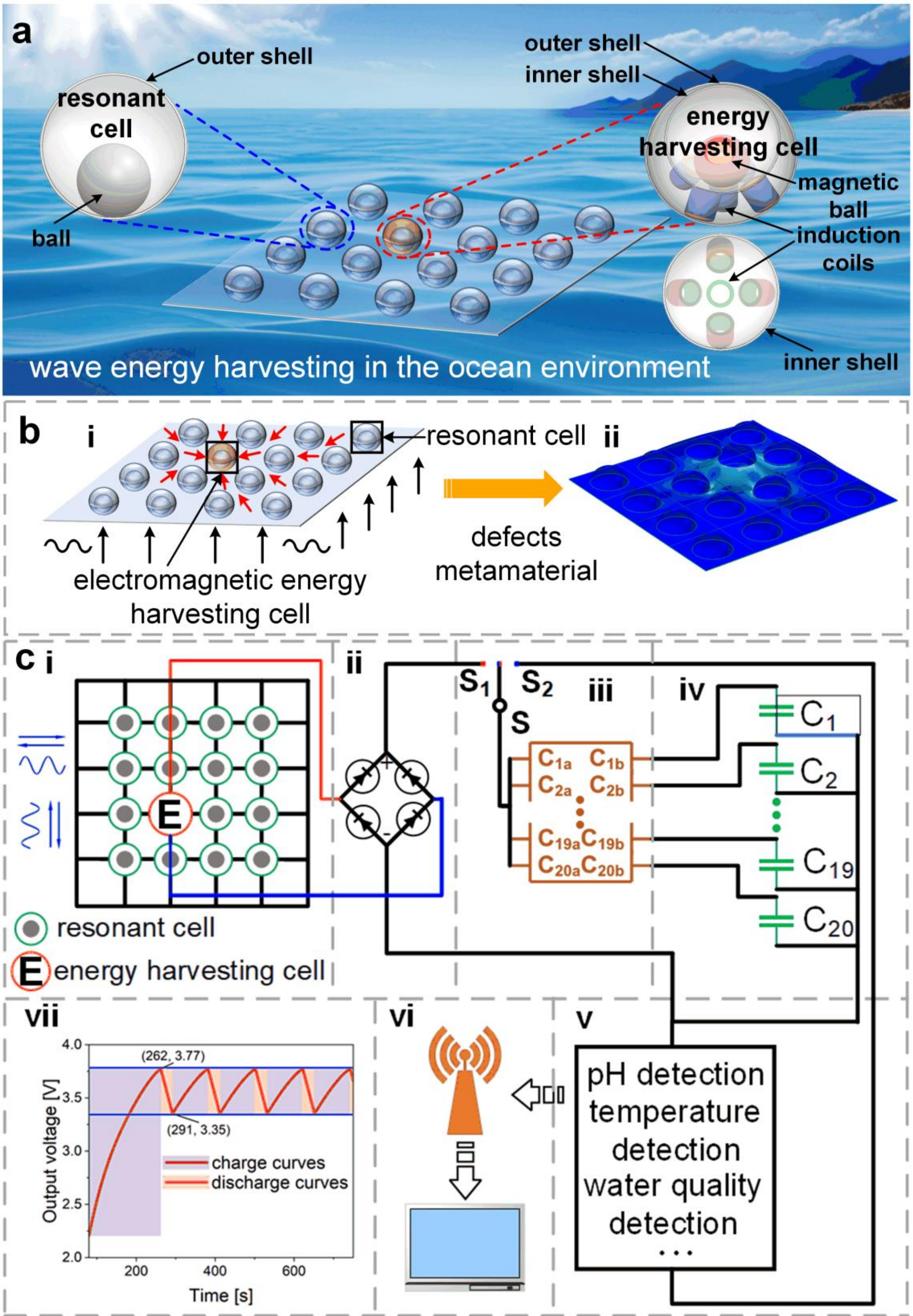

Fig. 1 Design diagram of wave energy harvesting and self-powered health monitoring system in OIoT. a. schematic of a metamaterial energy harvester harvesting wave energy from the ocean environment. The red dashed circle illustrates the electromagnetic energy harvesting cell and the blue dashed circle illustrates the resonant cell; b: (i) Schematic of the energy concentration

phenomenon of the metamaterial with defects under wave excitation; (ii) Simulated displacement clouds of metamaterial plates with point defects when excited by ocean waves, c. schematic design of a self-powered ocean environmental health monitoring system: (i) high-density wave energy harvesting metamaterial panels. The green circle illustrates the resonant cell and the red circle illustrates the energy harvesting cell, (ii) rectifier module (AC→DC); (iii) Series/parallel conversion module for energy storage elements. (S is a single-patch double-throw switch (ADG719-EP) integrated into the circuit to achieve series/parallel conversion of the energy storage element. When S_1 is closed, the capacitors are connected in parallel and the energy storage element is charged; when S_2 is closed, the capacitors are connected in series and the energy storage element is discharged); (iv) energy storage module; (v) environmental condition monitoring module (e.g. pH, temperature, and water quality); (vi) monitored information receiving module; and (vii) charge/discharge curves of the energy storage modules;

On Page 17

The rolling magnetic ball in the nonlinear electromagnetic energy harvester causes a small rotational jitter around a wave at a = 0.5g and f = 2 Hz, as a stable position when the energy-harvesting metamaterial plate is excited, as illustrated in Fig. 3c(iii).

Reviewer #2:

This paper presents the development of a robust, waterproof, floatable metamaterial energy harvesting device. The authors comprehensively discussed the development process, covering design, theoretical aspects, and testing. The work presented is of significance to the energy harvesting field and the paper holds potential for publication in Nature Communications; however, a revision is required and several areas need to be addressed, as outlined below.

Response: Thank you for your detailed review of our manuscript. The constructive comments are invaluable in improving the quality of our article. We have reviesed the paper accordingly. The changes are highlighted in blue in the revised document. Please find the following point-by-point responses and revisions/corrections.

(1) The paper's introduction is well-written, addressing various points. However, the results section appears to redundantly review aspects previously covered in the introduction. It is suggested to review and revise the first seven lines of the first paragraph in the Results section to avoid redundancy.

Response: We have revised the text to avoid redundancy. The change addressing the issues mentioned by the reviewer is outlined below.

Changes:

On Page 5

~~Various sensors are crucial to building the OIoT[1–3] to monitor the ocean environment, including temperature, nitrogen and oxygen content, and ocean organisms. Several methods, including solar panels [12–14] and wind turbines [15,16], can supply energy to ocean sensors. However, these energy supply methods often entail high costs, generate chemical pollution, and exhibit poor ability to cope with extreme weather. Considering factors such as cost and pollution, using the energy concentration property of metamaterials to harvest wave energy from the ocean is a potential solution for achieving a low-cost, highly reliable power supply to sensors. A schematic of the energy-harvesting process of a metamaterial energy-harvesting device in an ocean wave environment is shown in Fig. 1a.~~The design of a self-powered ocean environmental health monitoring system that converts ocean wave energy into electrical energy is illustrated in Fig. 1.

(2) Adding a paragraph to elaborate on how energy is concentrated in the defective location and the mechanisms behind it would enhance the paper.

Response: We have added paragraphs explaining how the energy is concentrated at the defect location and describing the mechanism. The changes addressing the issues mentioned by the reviewer are outlined below.

Changes:

On Page 5

The metamaterial plate consists of 4 × 4 cells (scalable), including 15 resonant cells without energy harvesting capability and 1 energy harvesting cell, as shown in Fig. 1a. The ball-rolling resonant cells of the periodic array regulate the propagation of elastic waves throughout the metamaterial plate. When the elastic wave propagates in the metamaterial, the energy harvesting cell at the defect is different from that of the entire periodic array, i.e., a local resonance is formed at the defect location, which limits the elastic wave to the defect location and generates a high-energy-density region to realize efficient harvesting of vibration energy.

(3) Clarify how the results in Fig 1b were modeled and how the metamaterial with defects was fabricated.

Response: We have discussed Fig. 1b further in the article and have described how the energy harvesting device was modeled and fabricated in the appendix. The change to the issues mentioned by the reviewer is listed below.

Changes:

On Page 5

Fig. 1b(i) illustrates the energy concentration characteristics of defective metamaterials under wave excitation, where the excitation of the metamaterials is concentrated at the defect location to generate a high-energy density zone. The displacement cloud of a metamaterial plate with point defects when subjected to wave excitation is modelled by finite element method as shown in Fig. 1b(ii). The energy concentrates per unit area at the location of the defects, resulting in an increase in displacement and more energy at the defect location when the metamaterial plate is subjected to out-of-plane excitation.

On Page 27

Manufacture of the Metamaterial with Defects

To fabricate point-defect metamaterials with energy-concentrating effects, the manufacturing processing of 3D-printing metamertial was employed. Firstly, the resonant cell was fabricated by combining one shell and one free-rolling ball. Then the produced resonant cells were periodically arrayed on a substrate to constitute a metamaterial with a low-frequency local resonant band gap. Then, one of the resonant cells was selected as the energy harvesting cell, which was modified by adding an inner shell, placing a free-rolling magnetic ball inside the inner shell and fixing five series-connected induction coils outside the inner shell. The energy harvesting cell had the same shell diameter compared with other resonant cells. The produced point-defect metamaterial exhibited the energy concentration effect.

(4) The details of the electromagnetic energy harvesting ball cell in CADs (Figures 1, 2, 3, etc.) lack clarity. Consider providing a better image or a separate figure to discuss the orientation of the ball and its poles against the coils. Include information on coil characteristics, orientation, distance between coils, magnetic ball movement and its magnetic strength. Describe the law governing voltage generation and provide details on sphere diameters.

Response: We have added further details on the rolling ball energy harvesting cell. The change to the issues mentioned by the reviewer is below.

Changes:

On Page 5

The red dashed circle represents the electromagnetic energy harvesting cell (active cell), which mainly consists of the outer shell, the inner shell, the magnetic ball, and the five series-connected induction coils solidly attached to the inner shell, whereas all the other cells on the plane are passive cells (with no energy harvesting capability), which consist of the outer shell and the resonant ball as shown by the blue dashed circle. as shown in Fig. 1a.

On Page 7

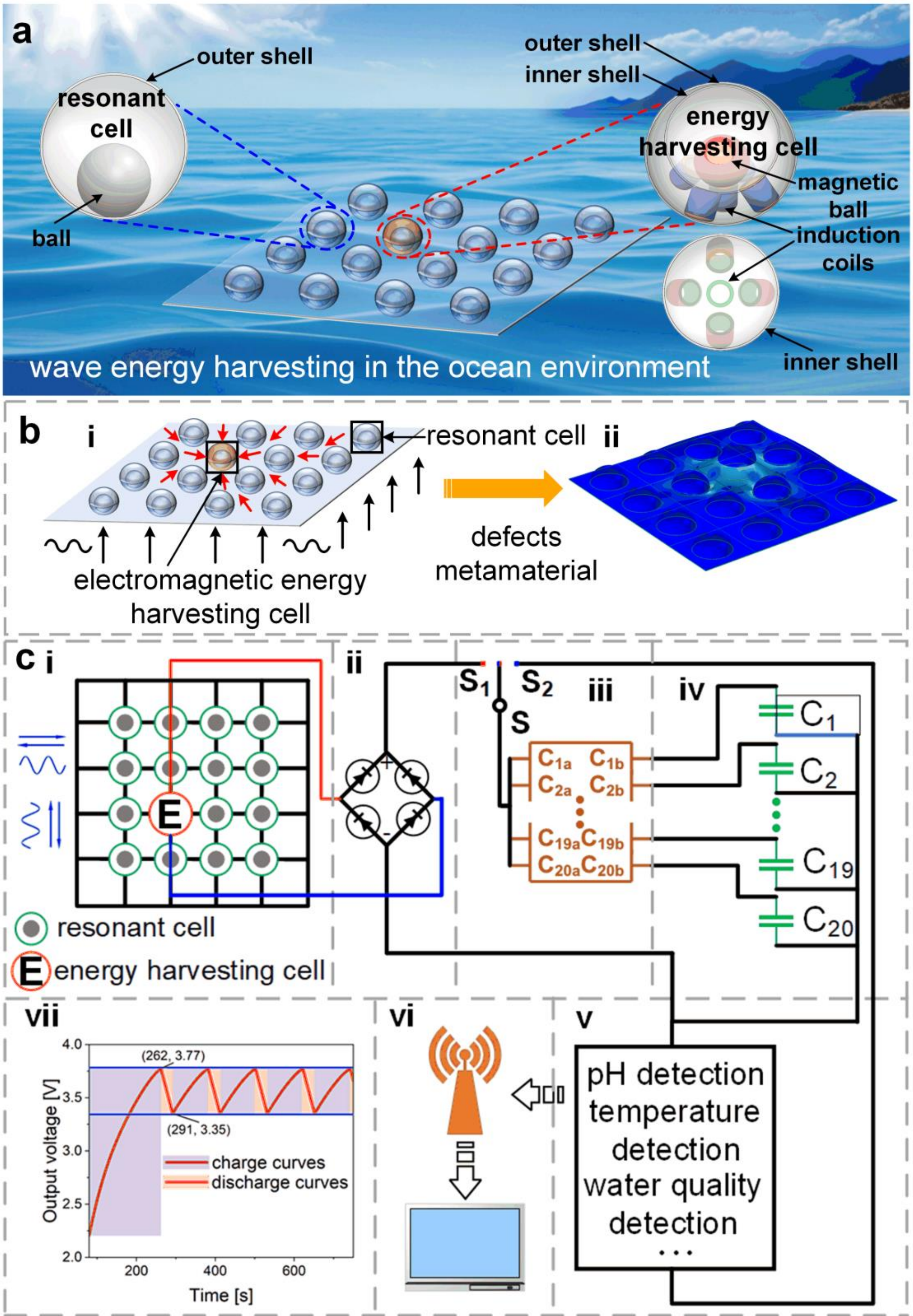

Fig. 1 Design diagram of wave energy harvesting and self-powered health monitoring system in OIoT. a. schematic of a metamaterial energy harvester harvesting wave energy from the ocean environment. The red dashed circle illustrates the electromagnetic energy harvesting cell and the blue dashed circle illustrates the resonant cell; b: (i) Schematic of the energy concentration phenomenon of the metamaterial with defects under wave excitation; (ii) Simulated displacement

clouds of metamaterial plates with point defects when excited by ocean waves, c. schematic design of a self-powered ocean environmental health monitoring system: (i) high-density wave energy harvesting metamaterial panels. The green circle illustrates the resonant cell and the red circle illustrates the energy harvesting cell, (ii) rectifier module (AC→DC); (iii) Series/parallel conversion module for energy storage elements. (S is a single-patch double-throw switch (ADG719-EP) integrated into the circuit to achieve series/parallel conversion of the energy storage element. When S_1 is closed, the capacitors are connected in parallel and the energy storage element is charged; when S_2 is closed, the capacitors are connected in series and the energy storage element is discharged); (iv) energy storage module; (v) environmental condition monitoring module (e.g. pH, temperature, and water quality); (vi) monitored information receiving module; and (vii) charge/discharge curves of the energy storage modules;

On Page 8

Table1 shows the physical parameters of the metamaterial resonant cell and the energy harvesting cell at the defect location.

On Page 10

Table 1. Physical parameters of the metamaterial resonant cell and energy harvesting cell

Item	Notation [unit]	Value
Metamaterials resonant cell		
Length	l_1[m]	0.06
Width	l_2[m]	0.06
Height	h[m]	0.001
Density of the plate	ρ_p[kg/m^3]	2100
Young's modulus of the plate	E_p[Pa]	7×10^8
Poisson’s ratio of the plate	ν_p	0.29
Radius of the outer shell	R_b[m]	0.04
Density of the rolling ball	ρ_r[kg/m^3]	7800
Young's modulus of the rolling ball	E_r[Pa]	2.1×10^{11}
Poisson’s ratio of the rolling ball	ν_r	0.3
Radius of the rolling ball	R_r[m]	0.0075
Energy harvesting cell at the defect location		
Induction coil (enameled copper wire)		
Induction coil resistance	R_L[Ω]	0.017
Inductor	L_{ind}[mH]	2
Turns of coil	n	200×5
Rolling magnetic balls (NdFeB)		
Radius of the magnetic ball	R_m[mm]	7.5
Magnetic flux density	B[mT]	345
Radius of the shell	R[mm]	20
Radius of the inner shell	Rs[mm]	15

(5) Give detailed information about the charging and discharging series/parallel series of capacitors, including layout, capacitor sizes, and control method of switches S1 and S2.

Response: We have further explained in the article the series-parallel conversion of the energy storage module, the type of capacitor, and the control method of switch S. The change to the issues mentioned by the reviewer is below.

Changes:

On Page 7, Fig. 1c(iii)

(iii) Series/parallel conversion module for energy storage elements. (S is a single-patch double-throw switch (SPDT, ADG719-EP) integrated into the circuit to achieve series/parallel conversion of the energy storage element. When S_1 is closed, the capacitors are connected in parallel and the energy storage element is charged. When S_2 is closed, the capacitors are connected in series and the energy storage element is discharged). This series/parallel coversion modulue allows the system to be able to charge the storage at low voltages and supply power to sensing subsystems at higher voltages, enhancing the energy harvesting capability.

On Page 6

As shown in Fig. 1c(iii), the design in this paper adds a new conversion module before the energy storage module, which is used to solve the problem of a single capacitor's low energy storage voltage that cannot drive the monitoring module. The electromagnetic energy harvester can charge multiple storage capacitors at the same time when connected in parallel, and the storage capacitors can output a high voltage when connected in series. Switch S is a single-patch, double-throw (ADG719-EP) switch that is controlled by a chip on the microcontroller. The capacitors (0.1F, 5.5V) are part of a series/parallel conversion module, which comprises multiple double-patch, double-throw (SGM7222YMS10/TR) chips integrated into the microcontroller. When the energy storage module is charging, S_1 is closed, creating a parallel connection between the capacitors. Conversely, when the energy storage module is discharging, S_2 is closed, forming a series connection between the capacitors, providing the monitoring module with a 3.3 V DC voltage.

(6) In line 114, specify the unit of the plate size.

Response: We have added the dimensional units of the metamaterial plates. The changes are listed below.

Changes:

On Page 8

The energy harvesting metamaterial plate, comprising 4 × 4 local resonance cells (0.06 m×0.06 m each), is shown in Fig. 2a.

(7) Discuss the mechanism and role of rolling balls in activating defective inductive balls.

Response: We have added the mechanism and role of rolling balls in activating the defect state properties of metamaterials in the revised manuscript. Below are the modifications addressing the reviewer's comment.

Changes:

On Page 5

The ball-rolling resonant cells of the periodic array tune the propagation of elastic waves in the metamaterial plate. When the elastic wave propagates in the metamaterial, the resonant cell at the defect is different from that of the entire periodic array, i.e., a local resonance is formed at the defect location, which limits the elastic wave to the defect location and generates a high-energy-density region to realize efficient harvesting of vibration energy.

(8) Clarify the information presented in Table 1, specifying whether it pertains to the plate or the energy harvesting cell. If the latter, provide details on the ball's dimensions. If the former, explain why the plate is only 6 cm long.

Response: We have revised this typo-thank you. The 6 cm long in Table 1 is the length of the metamaterial cell substrate. Below are the modifications addressing the reviewer's comment.

Changes:

On Page 10

Table 1. Physical parameters of the metamaterial resonant cell and the energy harvesting cell

Item	Notation [unit]	Value
Metamaterials resonant cell		
Length	l_1[m]	0.06
Width	l_2[m]	0.06
Height	h[m]	0.001
Density of the plate	ρ_p[kg/m^3]	2100
Young's modulus of the plate	E_p[Pa]	7×10^8
Poisson's ratio of the plate	ν_p	0.29
Radius of the outer shell	R_b[m]	0.04
Density of the rolling ball	ρ_r[kg/m^3]	7800
Young's modulus of the rolling ball	E_r[Pa]	2.1×10^{11}
Poisson's ratio of the rolling ball	ν_r	0.3
Radius of the rolling ball	R_r[m]	0.0075
Energy harvesting cell at the defect location		
Induction coil (enameled copper wire)		
Induction coil resistance	R_L[Ω]	0.017
Inductor	L_{ind}[mH]	2
Turns of coil	n	200×5
Rolling magnetic balls (NdFeB)		
Radius of the magnetic ball	R_m[mm]	7.5
Magnetic flux density	B[mT]	345
Radius of the shell	R[mm]	20
Radius of the inner shell	Rs[mm]	15

(9) Provide a comprehensive description of the graph in Figure 2d, labeling all curves.

Response: We have labeled all the curves in Fig. 2d and further explained Fig. 2d. The change to the issues mentioned by the reviewer is below.

Changes:

On Page 9

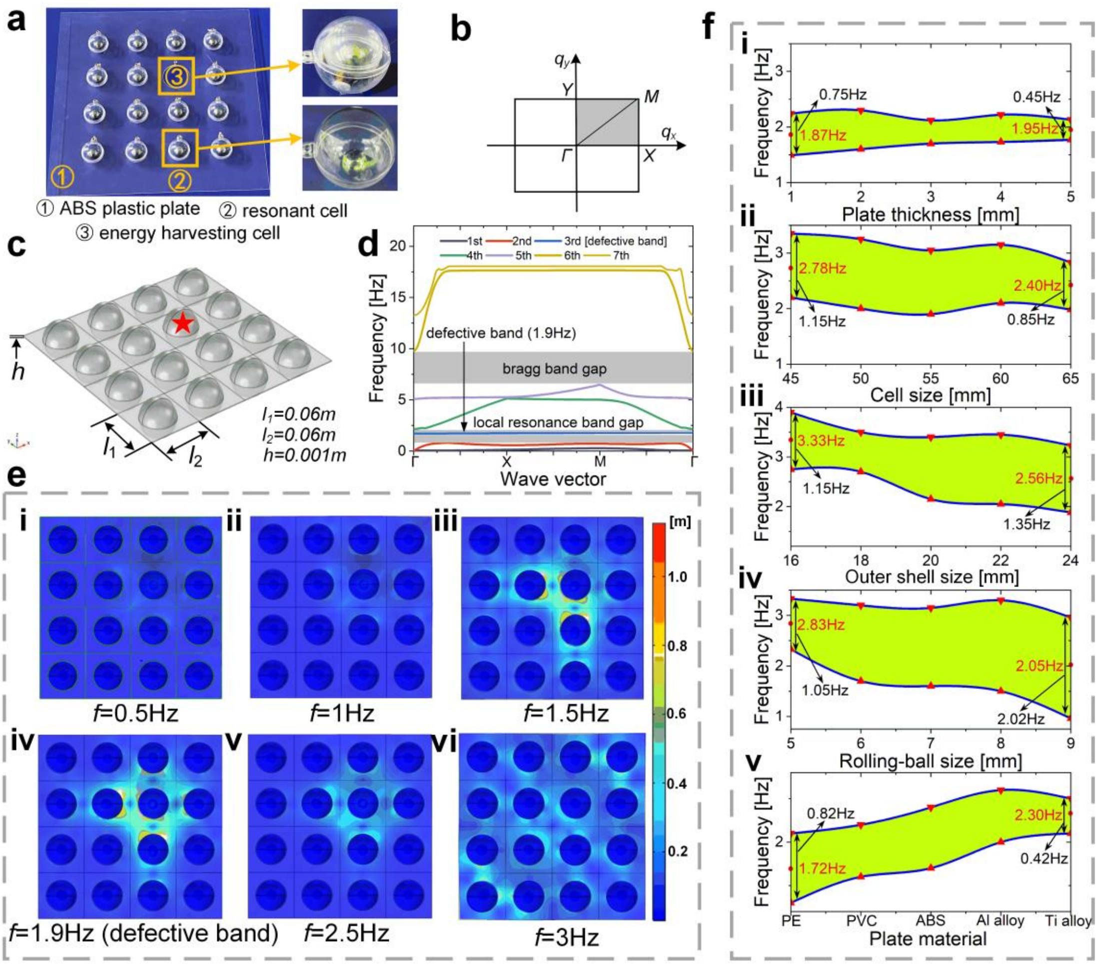

Fig 2. Finite element analysis of energy-harvesting metamaterials. a. High-density energy-harvesting metamaterial plates (0.3m×0.3m) based on defect characteristics: ① ABS plastic plate; ② resonant cell; ③ energy harvesting cell. b. simple Brillouin region for two-dimensional metamaterials; c. finite element model of a defective metamaterial plate; d. theoretical band structures of defective metamaterial plates; e. displacement clouds when an acceleration excitation a = 1g is applied to the lower surface of a metamaterial plate containing a point defect: (i) f = 0.5 Hz; (ii) f = 1 Hz; (ii) f = 1.5 Hz; (iv) f = 1.9 Hz (Defective band); (v) f = 2.5 Hz; (vi) f = 3 Hz;f. effect of geometrical parameters of high-density energy-harvesting metamaterial devices on the frequency range of defect bands: (i) plate thickness; (ii) cell size; (iii) outer shell size; (iv) rolling-ball size; (v) plate material.

On Page 10

The defect band in the energy band structure can be created by artificially introducing a defect cell (in this study, an energy harvesting cell) into the periodic array cell. The band gap containing the third-order eigenfrequency is the defect band introduced by this defect, as illustrated in Fig. 2d. Within the frequency range of this defect band, the elastic wave propagates through the metamaterial and concentrates at the defect location.

(10) For Figure 2f, which discusses several geometrical parameters affecting the frequency band, and Figure 2e, claiming optimal results at 1.9 Hz, disclose the specific geometrical values used in modeling for Fig. 2e.

Response: We have added the specific geometrical parameters of Fig. 2e in the revised manuscript. The change to the issues mentioned by the reviewer is below.

Changes:

On Page 8

Table1 shows the physical parameters of the metamaterial resonant cell and energy harvesting cell at the defect location.

On Page 10

Table 1. Physical parameters of the metamaterial resonant cell and energy harvesting cell

Item	Notation [unit]	Value
Metamaterials resonant cell		
Length	l_1[m]	0.06
Width	l_2[m]	0.06
Height	h[m]	0.001
Density of the plate	ρ_p[kg/m^3]	2100
Young's modulus of the plate	E_p[Pa]	7×10^8
Poisson's ratio of the plate	ν_p	0.29
Radius of the outer shell	R_b[m]	0.04
Density of the rolling ball	ρ_r[kg/m^3]	7800
Young's modulus of the rolling ball	E_r[Pa]	2.1×10^{11}
Poisson's ratio of the rolling ball	ν_r	0.3
Radius of the rolling ball	R_r[m]	0.0075
Energy harvesting cell at the defect location		
Induction coil (enameled copper wire)		
Induction coil resistance	R_L[Ω]	0.017
Inductor	L_{ind}[mH]	2
Turns of coil	n	200×5
Rolling magnetic balls (NdFeB)		
Radius of the magnetic ball	R_m[mm]	7.5
Magnetic flux density	B[mT]	345
Radius of the shell	R[mm]	20
Radius of the inner shell	Rs[mm]	15

(11) Specify the displacement unit in the vertical axis of Figure 2e.

Response: We have added the unit of the vertical axis of Fig. 2e. The change addressing the issues mentioned by the reviewer is outlined below.

Changes:

On Page 9

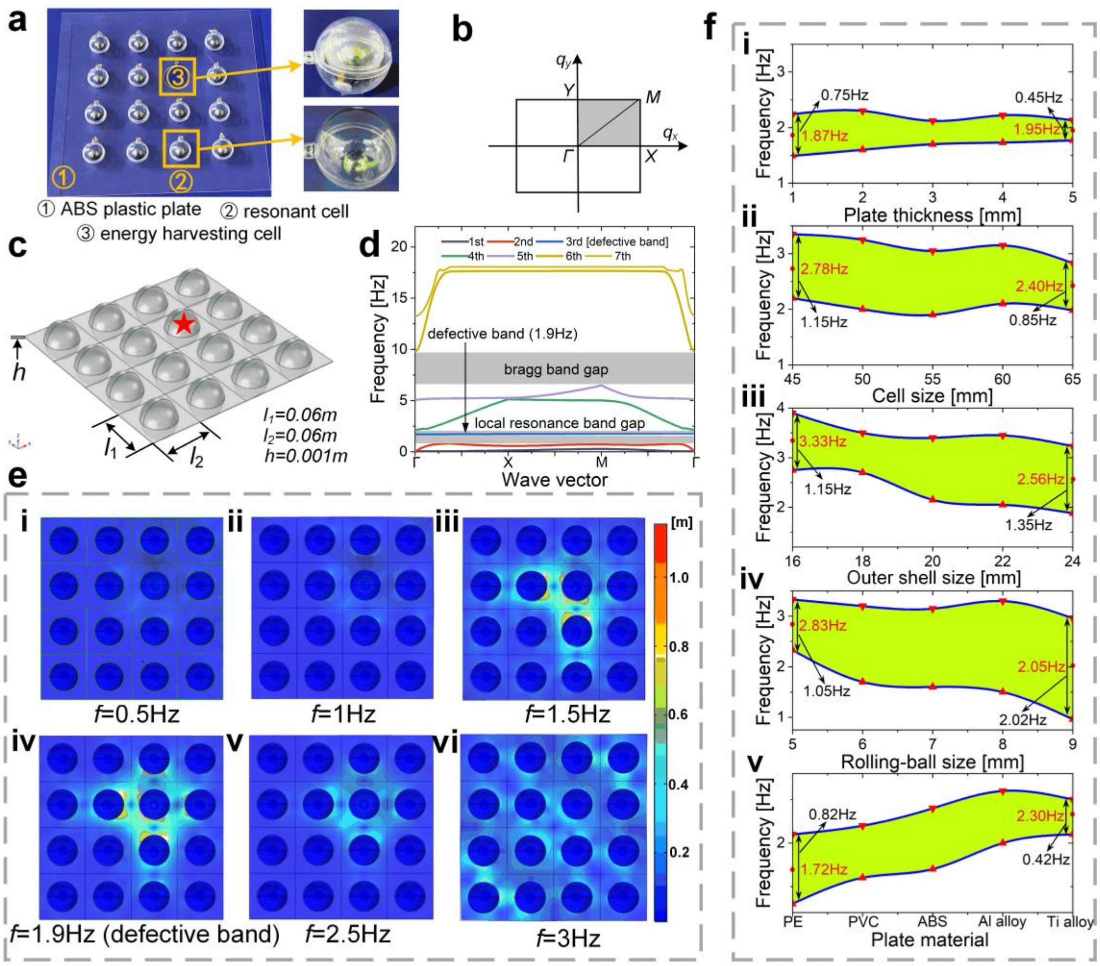

Fig 2. Finite element analysis of energy-harvesting metamaterials. a. High-density energy-harvesting metamaterial plates (0.3m×0.3m) based on defect characteristics: ① ABS plastic plate; ② resonant cell; ③ energy harvesting cell; b. simple Brillouin region for two-dimensional metamaterials; c. finite element model of a defective metamaterial plate; d. theoretical band structures of defective metamaterial plates; e. displacement clouds when an acceleration excitation *a* = 1g is applied to the lower surface of a metamaterial plate containing a point defect: (i) *f* = 0.5 Hz; (ii) *f* = 1 Hz; (ii) *f* = 1.5 Hz; (iv) *f* = 1.9 Hz (Defective band); (v) *f* = 2.5 Hz; (vi) *f* = 3 Hz; f. effect of geometrical parameters of high-density energy-harvesting metamaterial devices on the frequency range of defect bands: (i) plate thickness; (ii) cell size; (iii) outer shell size; (iv) rolling-ball size;(v) plate material.

(12) It seems that the material selected for the base plate will affect the frequency results and even the amplitude of the vibration in the defective location? Discuss why ABS was chosen for the base plate material and consider exploring other materials and their potential impact on frequency results. Are there any better materials for that? If so, what would be the results if they are used? It is understandable that the authors may not have tested other materials, but if would be great to have at least such a discussion.

Response: We have added a discussion of the various materials for metamaterial substrates. The metamaterial substrate affects the frequency range of the local resonance band. In the case of substrate materials that are strong enough to float on the surface of the sea, the ABS material can satisfy these requirements. The change addressing the issues mentioned by the reviewer is outlined below.

Changes:

On Page 9

The effect of energy-harvesting metamaterial plate materials on the local resonance band gap is discussed in Fig. 2f(v). The main considerations are Polyethylene (PE, E=1Gpa, ρ=0.9g/cm3), Polyvinyl Chloride (PVC, E=2Gpa, ρ=1.5g/cm3), Acrylonitrile Butadiene Styrene (ABS, E = 2.5 Gpa, ρ = 0.9g /cm3), Aluminum (Al alloy, E=72Gpa,ρ=2.7g/cm3), Titanium (Ti alloy, E=116Gpa, ρ=4.5g/cm3). According to the findings presented in Fig. 2f(v), the choice of the metamaterial plate material marginally influences the bandwidth and central frequency of the local resonance band gap. The band gap bandwidth for metamaterials with a non-metallic material substrate is 0.8 Hz, whereas that for those with a metallic material substrate is 0.5 Hz. However, the center frequency for band gaps using a metallic material substrate reaches 2.3 Hz, which exceeds the frequency range of ocean waves. Considering the buoyancy and strength requirements of wave energy harvesting devices, this study selects ABS as the optimal material for constructing the energy-harvesting device's plate. Therefore, a larger resonant mass results in a wider local resonant band gap and a wider frequency range for high-density energy harvesting of ocean wave energy. In summary, the criteria for the design of the metamaterial plane to achieve high-density energy harvesting include a thin substrate, a large cell, a heavy resonant mass and a low density and a high strength.

On Page 9

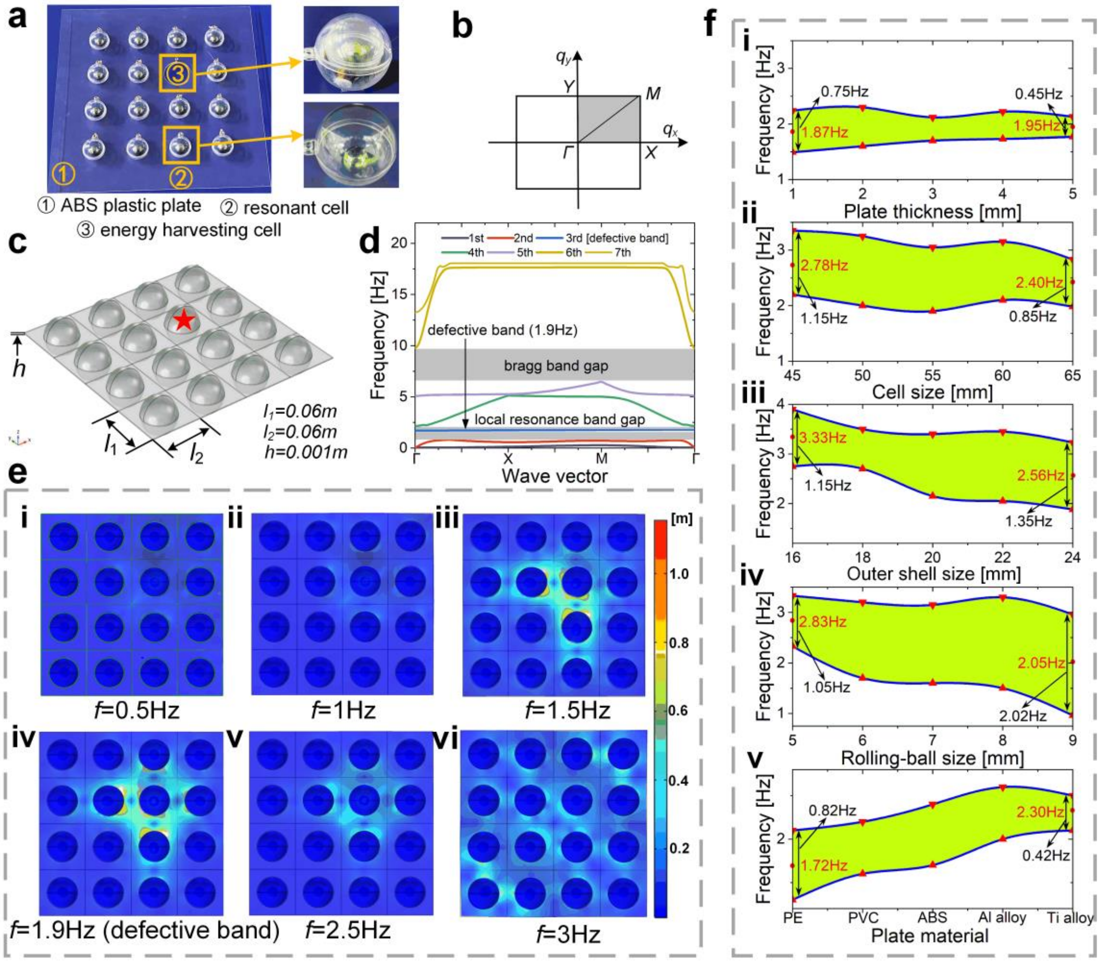

Fig 2. Finite element analysis of energy-harvesting metamaterials. a. High-density energy-harvesting metamaterial plates (0.3m×0.3m) based on defect characteristics: ① ABS plastic plate; ② resonant cell; ③ energy harvesting cell. b. simple Brillouin region for two-dimensional metamaterials; c. finite element model of a defective metamaterial plate; d. theoretical band structures of defective metamaterial plates; e. displacement clouds when an acceleration excitation a = 1g is applied to the lower surface of a metamaterial plate containing a point defect: (i) f = 0.5 Hz; (ii) f = 1 Hz; (ii) f = 1.5 Hz; (iv) f = 1.9 Hz (Defective band); (v) f = 2.5 Hz; (vi) f = 3 Hz; f. effect of geometrical parameters of high-density energy-harvesting metamaterial devices on the frequency range of defect bands: (i) plate thickness; (ii) cell size; (iii) outer shell size; (iv) rolling-ball size;(v) plate material.

(13) Add the typical frequency range of ocean waves and clarify the target values for the experiments.

Response: We have added wave spectra obtained from actual measurements to clarify the experimental target values in the article. Below are the modifications addressing the reviewer's comment.

Changes:

On Page 23

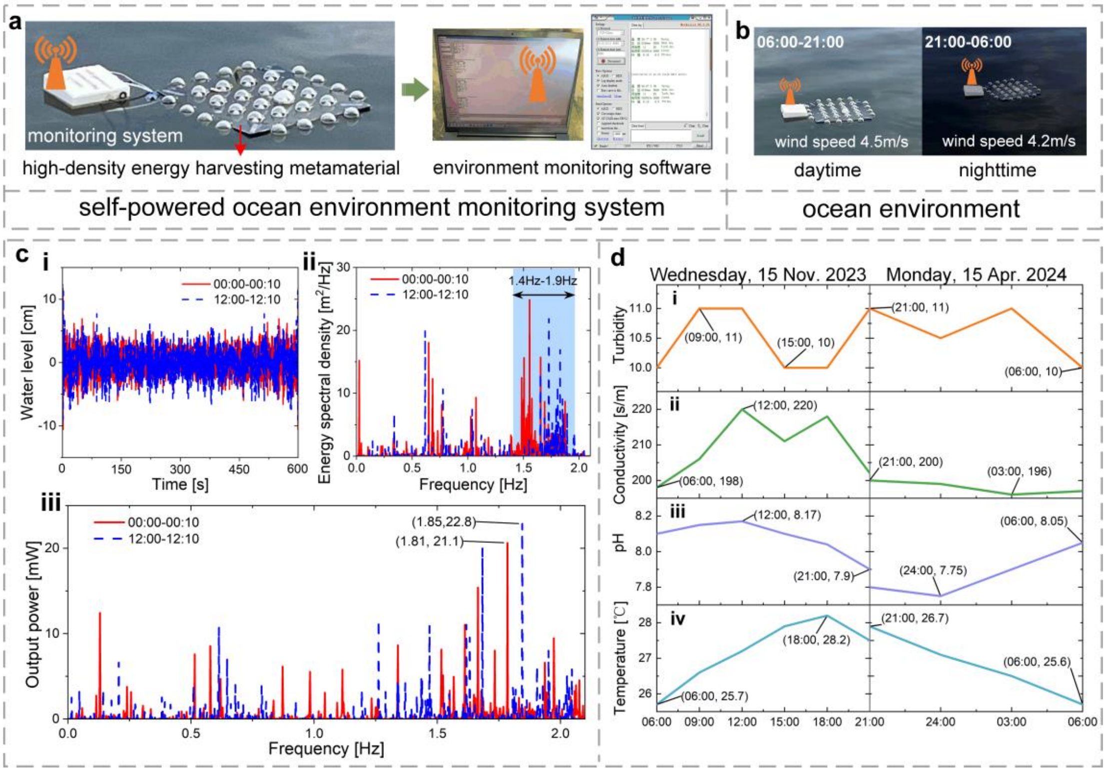

Fig. 5. Self-powered ocean environment monitoring system. a. Self-powered ocean environment monitoring system (High-density energy harvesting metamaterials and environmental monitoring software); b. Schematic diagram of the experiment in the ocean environment: daytime test environment (wind speed of 4.5 m/s) and nighttime test environment (wind speed of 4.2 m/s); c. Experimental results (red solid line: 00:00-00:10; blue dotted line: 12:00-12:10): (i) spectrum of wave levels; (ii) energy spectral density of the wave; (iii) Output power spectra of high-density energy harvesting metamaterials; d. real-time health monitoring results of the ocean environment in one day (24h): (i) turbidity, (ii) conductivity, (iii) pH, and (iv) temperature.

To clarify the target frequency of the metamaterial energy harvesting device for realizing the energy concentration phenomenon, the real-time wave height monitoring function of the energy harvesting device was used to derive the wave height monitoring data. The real ocean environment excitation has random spectrum featrure as shown in Fig. 5c(i and ii). (the red solid line is the instantaneous wave spectrum at 00:00-00:10 and the blue dashed line is the instantaneous wave spectrum at 12:00-12:10).The ocean wave frequencies are distributed within 0.1–2.1 Hz but are primarily concentrated in the frequency ranges of 0.5–1 Hz and 1.5–1.9 Hz. Therefore, the energy concentration frequency of the metamaterial energy harvesting device locates at those frequency ranges, resulting in better energy harvesting efficiency.

(14) Address the potential disparity between testing conducted on a standard shaker, where the plate is positioned on a horizontal shaker base during vibration, and the actual conditions of ocean waves impacting the plate's orientation. The testing scenario on a regular shaker, assuming a fixed orientation, may not precisely replicate the dynamic conditions experienced in the ocean. In reality, ocean waves can cause the plate to shift from a vertical to a horizontal orientation and vice versa. The significance of this discrepancy depends on whether the shaker base is rotatable. If the shaker base is rotatable, this concern may be mitigated. However, additional considerations arise concerning the plate's structure and the location of the energy harvesting cell. In the ocean, waves can approach the plate from any side or even from different sides along the same axis, potentially leading to asymmetry in cell exposure. How have you addressed or justified these factors in your testing methodology?

Response:

In the ocean wave environment simulation experiment, the metamaterial plate can move arbitrarily in the tank following the wave, and as the reviewer mentioned, the wave can apply excitation to the metamaterial from any side. In harsh ocean environments such as typhoons, the acceleration of waves is generally greater than 0.5g[64,65], which is related to many factors such as ocean depth, area, and wave period. The acceleration of waves is used as an index to distinguish stable and harsh ocean wave environments.In the simulation, the shaker base does not rotate, but the triaxial shaker used in the experiment can now be excited in any direction in the plane, and the direction of excitation of the shaker on the tank was not clearly described in the article. We have further explained how the excitation is applied to the tank in the simulation section. The change to the issues mentioned by the reviewer is below.

Changes:

On Page 14

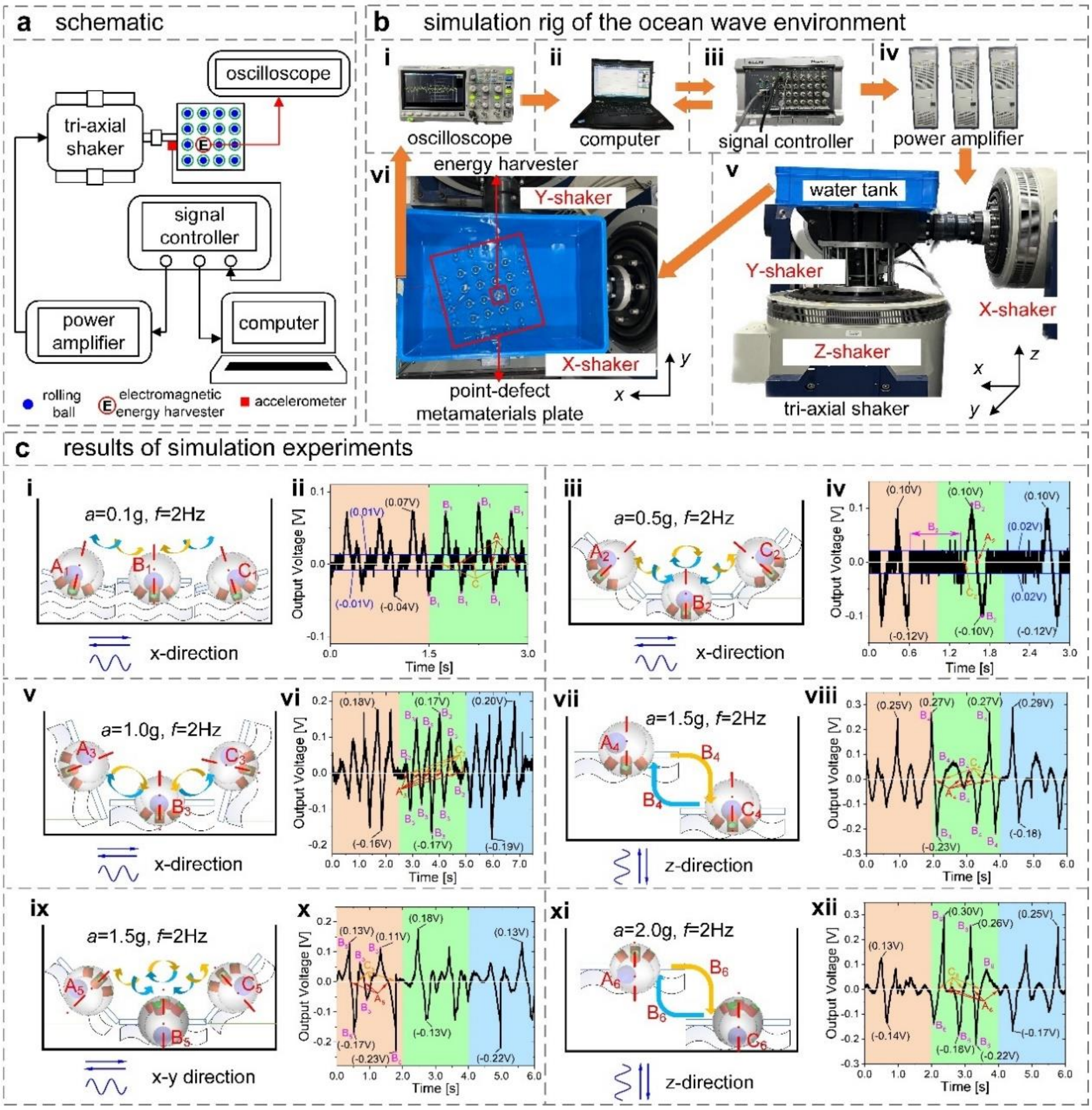

Fig 3. Experiments of the response of a high-density energy-harvesting metamaterial device under various wave size conditions. a. schematic of the experimental rig; b. photographs of the experimental rig: (i) oscilloscope, which shows the energy-harvesting metamaterial plate output voltage; (ii) computer; (iii) signal controller, which generates sinusoidal signals; (iv) power amplifier; (v) triaxial shakers that provide excitation in the *x*-, *y*- and *z*-directions; (vi) flume, which simulates the ocean wave environment; c. motion state analysis and output voltage of a rolling magnetic ball in a metamaterial energy-harvesting device under various wave conditions: (i), (ii): *a*

= 0.1 g, f = 2 Hz, x-direction excitation; (iii), (iv): a = 0.5 g, f = 2 Hz, x -direction excitation; (v), (vi): a =1.0 g, f=2Hz, x -direction excitation; (vii), (viii): a = 1.5 g, f = 2 Hz, z-direction excitation; when the energy harvesting metamaterial plate is in the multi-direction excitation state; (ix), (x): a = 1.5 g, f = 2 Hz, x -y-direction excitation, when the energy harvesting metamaterial plate is in the multi-direction excitation state; (xi), (xii): a =2.0 g, f = 2 Hz, z-direction excitation, when the energy harvesting metamaterial plate is in the overturning state; where (i)–(vi) simulate the motion state and energy output of the rolling ball in the metamaterial energy harvester in a steady wave environment, (vii)–(xii) simulate the motion state and energy output of the rolling ball in the metamaterial energy harvester in a harsh environment.

Table 2. Conditions of the ocean wave environment simulation experiments

Excitation acceleration[1] [g]	Excitation direction	Metamaterial plate	Simulation of the ocean wave environment
0.1	x-direction	no flip	stable
0.5	x-direction	no flip	stable
1	x-direction	no flip	harsh
1.5	z-direction	no flip	harsh
1.5	x-y direction	flip	harsh
2	z-direction	flip	harsh

[1] In harsh ocean environments such as typhoons, the acceleration of waves is generally greater than 0.5g[64,65], which is related to many factors such as ocean depth, area, and wave period. The acceleration of waves is used as an index to distinguish stable and harsh ocean wave environments.

On Page 16

In ocean environments, the energy harvesting device can experience asymmetric excitation from multiple directions, resulting in the flipping of the metamaterial energy harvesting device. Fig. 3c(ix) simulates a working condition in which the metamaterial energy harvesting device is subjected to simultaneous x-y multi-directional excitations in a flipped state. Observing the motion of the energy harvesting device reveals that this device undergoes a rotational motion while moving with the wave, and the rolling sphere also rotates along the inner wall of the shell when the rolling magnetic sphere is farther away from the induction coil, i.e., B_5-(yellow arrow)-A_5-(blue arrow)-B_5; B_5-(yellow arrow)-C_5-(blue arrow). In the process of movement, the speed of the rolling magnetic ball relative to the induction coil is maximum in the B5 state, resulting in the highest instantaneous output voltage of 0.23 V. Conversely, in the A_5 and C_5 states, the speed of the rolling magnetic ball relative to the induction coil is zero, leading to an instantaneous output voltage of 0. In the flip state, as shown in Fig. 3c(x), the output voltage of the metamaterial energy harvesting device decreases. The output voltage of the device in the flip state is 0.23 V. This simulation confirms that the device also exhibits good energy harvesting capability under asymmetric excitation.

(15) Discuss the implications if the ocean waves cause the plate to flip over. Do you anticipate similar results when the vibration is applied from the other side?

Response: The phenomenon of flipping over of the metamaterial plates occurs when ocean waves are sufficiently large. Therefore, we have added experiments on metamaterial plates in the overturned state when subjected to different wave excitations and analyzed the results of their kinematics and energy output. The change to the issues mentioned by the reviewer is below.

Changes:

On Page 13

Table 2 shows the applied conditions for simulating the types of ocean wave environments. The experiments revealed that when the tank's acceleration was less than 1g, small stable waves were generated. When the acceleration was 1g, large stable waves were generated. When the acceleration was greater than 1g, the waves became huge and broken. When the acceleration was greater than 2g, the waves significantly impacted the metamaterial energy harvesting device, occasionally causing the metamaterial plate to flip over. Thus, in this study, the simulated ocean waves under different excitations are classified as wave, large wave, and harsh wave. When the applied acceleration exceeds 2g, the wave impact on the water tank may cause the metamaterial fracture. Consequently, the maximum excitation acceleration is limited to 2g.

Table 2. Conditions of the ocean wave environment simulation experiments

Excitation acceleration[1] [g]	Excitation direction	Metamaterial plate	Simulation of the ocean wave environment
0.1	*x*-direction	no flip	stable
0.5	*x*-direction	no flip	stable
1	*x*-direction	no flip	harsh
1.5	*z*-direction	no flip	harsh
1.5	*x*-*y* direction	flip	harsh
2	*z*-direction	flip	harsh

[1] In harsh ocean environments such as typhoons, the acceleration of waves is generally greater than 0.5g[64,65], which is related to many factors such as ocean depth, area, and wave period. The acceleration of waves is used as an index to distinguish stable and harsh ocean wave environments.

On Page 18

In ocean environments, the energy harvesting device can be subjected to asymmetric excitation in multiple directions, resulting in the discovery of the flipping of the metamaterial energy harvesting device. Fig. 3c(ix) simulates an experiment in which the metamaterial energy harvesting device is subjected to simultaneous x-y multi-directional excitations in a flipped state. The motion of the energy harvesting device was observed, and it was found that the energy harvesting device made a rotational motion while moving with the wave, and the rolling sphere also made a rotational motion along the inner wall of the ball shell, when the rolling magnetic sphere was farther away from the induction coil, i.e., B_5-(yellow arrow)-A_5-(blue arrow)-B_5; B_5-(yellow arrow)-C_5-(blue arrow) -B_5. In the process of movement, the speed of the rolling magnetic ball relative to the induction coil is maximum in the B_5 state, and the instantaneous output voltage is the highest, 0.23 V; the speed of the rolling magnetic ball relative to the induction coil is zero in the A_5 and C_5 states, and the instantaneous output voltage is 0. The output voltage of the metamaterial energy harvesting device decreases in the flip state in Fig. 3c(x), and the output voltage of the metamaterial energy harvesting device in the flip state is 0.23 V. This simulation confirms that the device also exhibits good energy harvesting capability under asymmetric excitation.

Fig. 3c(xi) simulates the motion state and energy output capability of the energy harvesting metamaterial plate in the overturning state at ultra-large vertical excitation a = 2.0g. This simulated environment is an extremely harsh ocean wave environment when the metamaterial plate is also in the up and down state on the ocean wave surface and the rolling magnetic ball in the energy harvester is in the jumping state. The motion of the energy harvesting device can be observed in moments A_6 and C_6, where the rolling magnetic ball and the inductive coil are in a relatively stationary state, and the instantaneous output voltage response is 0, as shown in Fig. 3c(xii). At moment B_6, the rolling ball in the energy harvesting device is in a jumping state, and the relative velocity between the rolling magnetic ball and the inductive coil is maximum at this instant, and the output voltage reaches 0.3 V. Consequently, given that the excitation of the wave to the energy harvesting device is sufficiently large, the device still maintains a high energy output in the overturning state.

(16) Figure 5 discusses the results of the field testing. Provide a comprehensive discussion of the signal transmission system on the plate during field testing with the information such as power consumption, maximum transmission distance, the method of sensor measurement, and the connection of the energy harvester to sensors, etc. Is the system connected through wires? If so, how did you seal it against water?

Response: The wave energy harvesting metamaterial board is connected to the monitoring device with wires, and the two parts are sealed and waterproofed with hot melt adhesive. We have described in detail how the monitoring system is connected. The changes are listed below.

Changes:

On Page 19

In the test, the wave energy high-density energy harvesting device based on the defective state characteristics of metamaterials was connected to the monitoring device with wires, and the parts were sealed with hot melt adhesive to waterproof the system to ensure the hermeticity of the ocean environmental health detection system.

On Page 21

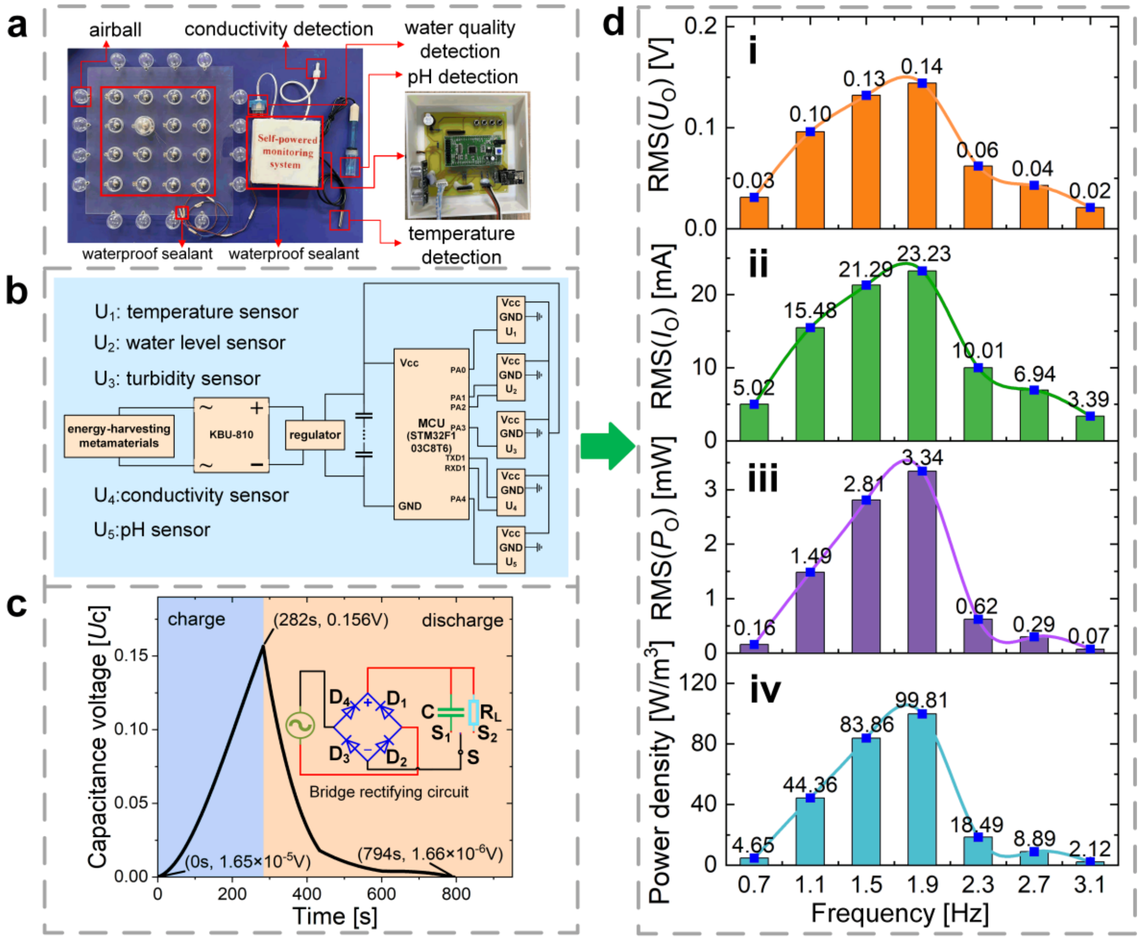

Fig 4. Schematic and characterization of a self-powered ocean environment monitoring system. a. schematic of the components of an ocean environment monitoring system for wave energy harvesting by a high-density energy-harvesting metamaterial device (the self-powered energy monitoring system is sealed with hot melt adhesive and the connections between the energy harvesting device and the detection system are waterproofed); b. schematic of self-powered ocean environment monitoring system circuits; c. capacitor charging and discharging experiments and results; d. output characterization of energy-harvesting metamaterials at different frequencies: (i) output voltage, (ii) output current, (iii) output power, and (iv) power density.

(17) Consider restructuring the paper, and section titles and order to enhance the flow. For example, arrange the theoretical aspect after introducing the design, followed by the description of the device, its fabricated parts, experimental details, and a comprehensive results discussion.

Response: We have reorganized the structure of the article to enhance the flow of the paper. The structure of the current article is as follows: first, the design of point defect metamaterial wave energy harvesting device and ocean environment health monitoring system is introduced. Then, the theoretical analysis of the point defect metamaterial wave energy harvesting device is conducted. Then, the excitation of various ocean wave environments on the energy harvesting device is simulated in the laboratory and the response is discussed. Finally, the usability of this self-powered energy ocean environment health monitoring system is verified by conducting real experiments in an ocean environment. The full results are discussed within each section, as required by the journal.

(18) Conclusions section is missing.

Response: According to the typical structures of published papers in Nature Communications, the conclusions in the manuscript are in the last paragraph of the discussion section. We have subdivided the conclusions to highlight them more clearly. The change to the issues mentioned by the reviewer is below.

Changes:

On Page 24

This study develops a high-density wave energy harvesting device using the defect state properties of metamaterials within the context of ocean wave energy applications. By incorporating energy harvesting defects within the artificial periodic array structure, ocean wave energy in a given area can be harvested more effectively. This involves channeling the wave energy into the energy harvesting device located at the metamaterial defects.

The findings demonstrate that for waves in the local resonance frequency range, an energy-harvesting device based on the defective state properties of metamaterials can efficiently harvest wave energy in the plane. Under different wave excitations, the electromagnetic energy-harvesting device in the metamaterial plate exhibits various states of motion: (a) Under very small wave excitation, the rolling magnetic ball within the electromagnetic energy-harvesting device undergoes a low-amplitude rolling motion along the shell and rotates around its center of mass. This indicates that the energy-harvesting device based on the defective state properties of the metamaterial produces induced voltages even with very small wave excitation; (b) under stable wave environment excitation, a "complex" nonlinear periodic phenomenon is generated, resulting in the rolling ball generating a peak induced voltage because of the accumulation of wave kinetic energy; (c) under harsh wave environment excitation, the rolling magnetic ball exhibits vigorous movement, while the metamaterial energy harvester demonstrates exceptional energy conversion capabilities. The output power and charge/discharge tests indicate that the energy-harvesting metamaterial device can convert wave energy into electrical energy for harvesting and use. To provide technical support for establishing an ocean environment monitoring network, an OIoT self-powered environment monitoring system cell is designed.

Reviewer #3:

A rolling ball water wave energy harvesting design based on the electromagnetic mechanism is introduced in this manuscript and the electrical outputs under various dynamics are shown. Although the design shows some outputs, there are several challenges with the novelty and contribution of the work and the justification for the need for such design.

Response: Thank you for your valuable comments. This study develops a wave energy harvesting device using the phenomenon of energy concentration in point defect metamaterials. This device can concentrate the in-plane wave kinetic energy within a rolling magnetic ball energy harvesting cell at the defect location to enable efficient harvesting of wave energy. Thus, this study develops a novel self-powered sensing node for the sensing network within the ocean IoT system, which for the first time uses the energy concentration effect of point-deficient metamaterials to efficiently harvest wave energy, thereby supplying electrical energy to the sensing nodes. The advantage of this design is that it concentrates energy harvesting at a point on a plane, thereby avoiding the issue of inconsistent AC phase that arises when multiple energy harvesters are placed across the plane.

Changes:

On Page 4

This study designs a novel self-powered sensing node for the sensing network in the ocean IoT system, which for the first time applies the energy concentration effect of point-deficient metamaterials for efficient wave energy harvesting to supply electrical energy of the sensing nodes for OIoT systems. This device is waterproof, corrosion-resistant, and unaffected by coatings, allowing for more effective harvesting and conversion of wave energy in extreme weather conditions. Compared with traditional ocean wave energy harvesters, the nonlinear electromagnetic energy harvesting device developed in this study offers the benefits of a simple structure, superior shock resistance, and cost-effectiveness. However, electromagnetic energy harvesting devices generate high-induced currents and low voltages, and the magnitude of the electrical output is affected by the rate of change of the magnetic flux. To address this challenge, this study pioneers the use of the unique defect state characteristics of metamaterials to harvest the scattered vibration energy within the oceam wave environment at the defect location of the metamaterials. The advantage of this design is that it centralizes energy harvesting at a point on a plane, thereby avoiding the issue of inconsistent AC phase that arises when multiple energy harvesters are placed across the plane.

(1) The design seems to be simplistic considering a moving magnet above some coils and then multiplying it into multiple units which would provide some small outputs under motions and thus, the novelty in the design is not significant enough.

Response: The energy harvesting device designed herein is not a periodic arrangement of electromagnetic rolling ball energy harvesters, but rather an electromagnetic rolling ball energy harvester placed in the periodic array of rolling ball resonance cells (not harvesters). The metamaterial plate consists of 4 × 4 cells (scalable), including 15 resonant cells without energy harvesting capability and 1 energy harvesting cell, as shown in Fig. 1a. The periodic array of ball resonators (not energy harvesters) provides a low-frequency local resonance bandgap in which the wave energy of the plate plane can be concentrated at the defect location, where the solo electromagnetic ball energy harvester is located, within the frequency range of the local resonance bandgap. This device achieves efficient harvesting of wave energy while avoiding the energy dissipation phenomenon that occurs when the phases of multiple harvesting cells are not uniform. Thus, this study develops a novel node for the sensing network within the ocean IoT system, which for the first time uses the energy concentration effect of point-defect metamaterials to efficiently harvest wave energy, thereby supplying electrical energy to the sensing nodes.

Changes:

On Page 4

This study designs a novel self-powered sensing node for the sensing network in the ocean IoT system, which for the first time applies the energy concentration effect of point-deficient metamaterials for efficient wave energy harvesting to supply electrical energy of the sensing nodes for OIoT systems.

On Page 8

A finite element schematic of the 4×4 periodic array of the rolling-ball resonator metamaterial plate is illustrated in Fig. 2c. The location of the red pentagram in Fig. 2c signifies the location of the point defect, where the rolling-ball energy harvester from Fig. 1b(i) is positioned to capture the concentrated vibration energy inside the plate. To simulate wave excitation to the plate, a vertical surface excitation (a = 1g) is applied to the lower surface of the metamaterial plate, and the response generated by this excitation is detected at the defect location. This study creates defective bands within the local resonance bandgap to achieve metamaterials with energy-concentrating characteristics at ultra-low frequencies. Fig. 2d illustrates the theoretical band structures of the point-defect nonlinear local resonance metamaterial. The defect band in the energy band structure can be created by artificially introducing a defect cell (in this study, an energy harvesting cell) into the periodic array cell. The band gap containing the third-order eigenfrequency is the defect band introduced by this defect, as illustrated in Fig. 2d. Within the frequency range of this defect band, the elastic wave propagates through the metamaterial and concentrates at the defect location. The metamaterial exhibits a local resonance band gap at low frequencies (0.9–2 Hz) and a Bragg band gap at higher frequencies (6.7–9.6 Hz). In-plane vibrations of the metamaterial plate are suppressed in the frequency range of the band gap. In particular, the in-plane vibrations of the plate are concentrated at the location of the point defect within the frequency range of the local resonance bandgap (0.9–2 Hz), creating a high-energy-density region.

The displacement cloud of the metamaterial plate in the low-frequency range (0.5–3 Hz) is illustrated in Fig. 2e. Figs. 2e(i), 2e(v), and 2e(vi) are outside the frequency range of the local resonance bandgap, whereas Figs. 2e(ii), Fig. 2e(iii), and 2e(iv) fall within the frequency range of the local resonance bandgap. The wave excitation is vertical to the defective metamaterial plate. From the displacement cloud, the resonant balls in each cell roll along the sphere cavities when the metamaterial plate is excited by waves, converting the out-of-plate excitation into in-plate excitation, which is concentrated at the energy harvesting device at the defect location, generating a high-energy-density region at the defect location. A limitation of this design is that the combination of vertical and lateral excitation could result in mistuning of the defect location because of the presence of lateral motion breaking the symmetry. Regarding the metamaterial energy concentration, the best results are achieved when the surface excitation frequency is 1.9 Hz (defective band). This establishes a theoretical basis for subsequently placing a nonlinear electromagnetic energy harvester at the defect location of the metamaterial plate to achieve high-density energy harvesting.

On Page 9

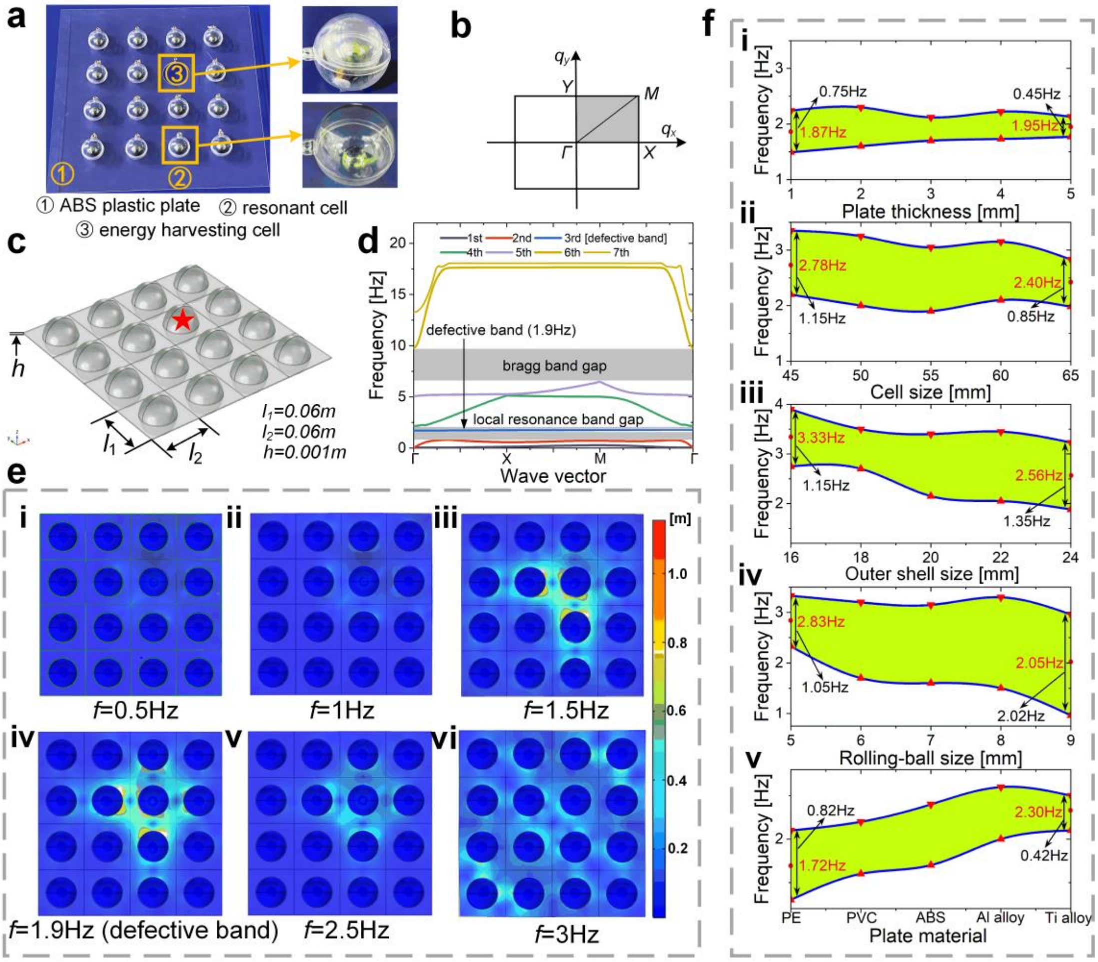

Fig 2. Finite element analysis of energy-harvesting metamaterials. a. High-density energy-harvesting metamaterial plates (0.3m×0.3m) based on defect characteristics: ① ABS plastic plate; ② resonant cell; ③ energy harvesting cell. b. simple Brillouin region for two-dimensional metamaterials; c. finite element model of a defective metamaterial plate; d. theoretical band structures of defective metamaterial plates; e. displacement clouds when an acceleration excitation a = 1g is applied to the lower surface of a metamaterial plate containing a point defect: (i) f = 0.5 Hz; (ii) f = 1 Hz; (ii) f = 1.5 Hz; (iv) f = 1.9 Hz (Defective band); (v) f = 2.5 Hz; (vi) f = 3 Hz; f. effect of geometrical parameters of high-density energy-harvesting metamaterial devices on the frequency range of defect bands: (i) plate thickness; (ii) cell size; (iii) outer shell size; (iv) rolling-ball size; (v) plate material.

(2) The efficient power management given the random nature of water wave motions and multiple units is a big concern and providing a stable output would be a big challenge given the use of complicated electronics would degrade the small output of the system and would not be justified.

Response: The metamaterial wave energy harvesting device proposed in this study has only one electromagnetic energy harvesting cell, so only the energy management for this energy harvesting cell is required. The presented point defect metamaterial energy harvesting device can concentrate the dispersed energy from the ocean wave surface, thereby avoiding the issue of inconsistent AC phase that arises when multiple energy harvesters are placed across the plane. The power management circuit used in this system is not complex as well, since most of them are well integrated.

Changes:

On Page 6

The design of the self-powered ocean environmental health monitoring system is shown in Fig. 1c. Figs. 1c (i) and (ii) illustrate the wave kinetic energy harvesting and conversion modules. As illustrated in Fig. 1c(i), an energy-harvesting metamaterial device is placed on the sea surface and driven via the kinetic-potential energy change of wave undulations to convert wave energy into electrical energy. As illustrated in Fig. 1c(ii), the alternating current (AC) is then converted to direct current (DC) using the rectifier module. As shown in Fig. 1c(iii), the design in this paper adds a new conversion module before the energy storage module, which is used to solve the problem of a single capacitor's low energy storage voltage that cannot drive the monitoring module. The electromagnetic energy harvester can charge multiple storage capacitors at the same time when connected in parallel, and the storage capacitors can output a high voltage when connected in series. Switch S is a single-patch, double-throw (ADG719-EP) switch that is controlled by a chip on the microcontroller. The capacitors (0.1F, 5.5V) are part of a series/parallel conversion module, which comprises multiple double-patch, double-throw (SGM7222YMS10/TR) chips integrated into the microcontroller. When the energy storage module is charging, S_1 is closed, creating a parallel connection between the capacitors. Conversely, when the energy storage module is discharging, S_2 is closed, forming a series connection between the capacitors, providing the monitoring module with a 3.3 V DC voltage. The energy storage module, where several capacitors provide sufficient driving voltage, is illustrated in Fig. 1c(iv). Fig. 1c(v) illustrates the ocean environment monitoring module that transmits the monitored data via the wireless module to the receiver module in Fig. 1c(vi). The charging and discharging curves of the energy storage module, which exhibit a cyclic charging and discharging phenomenon after the initial charging is completed, are illustrated in Fig. 1c(vii).

On Page 7

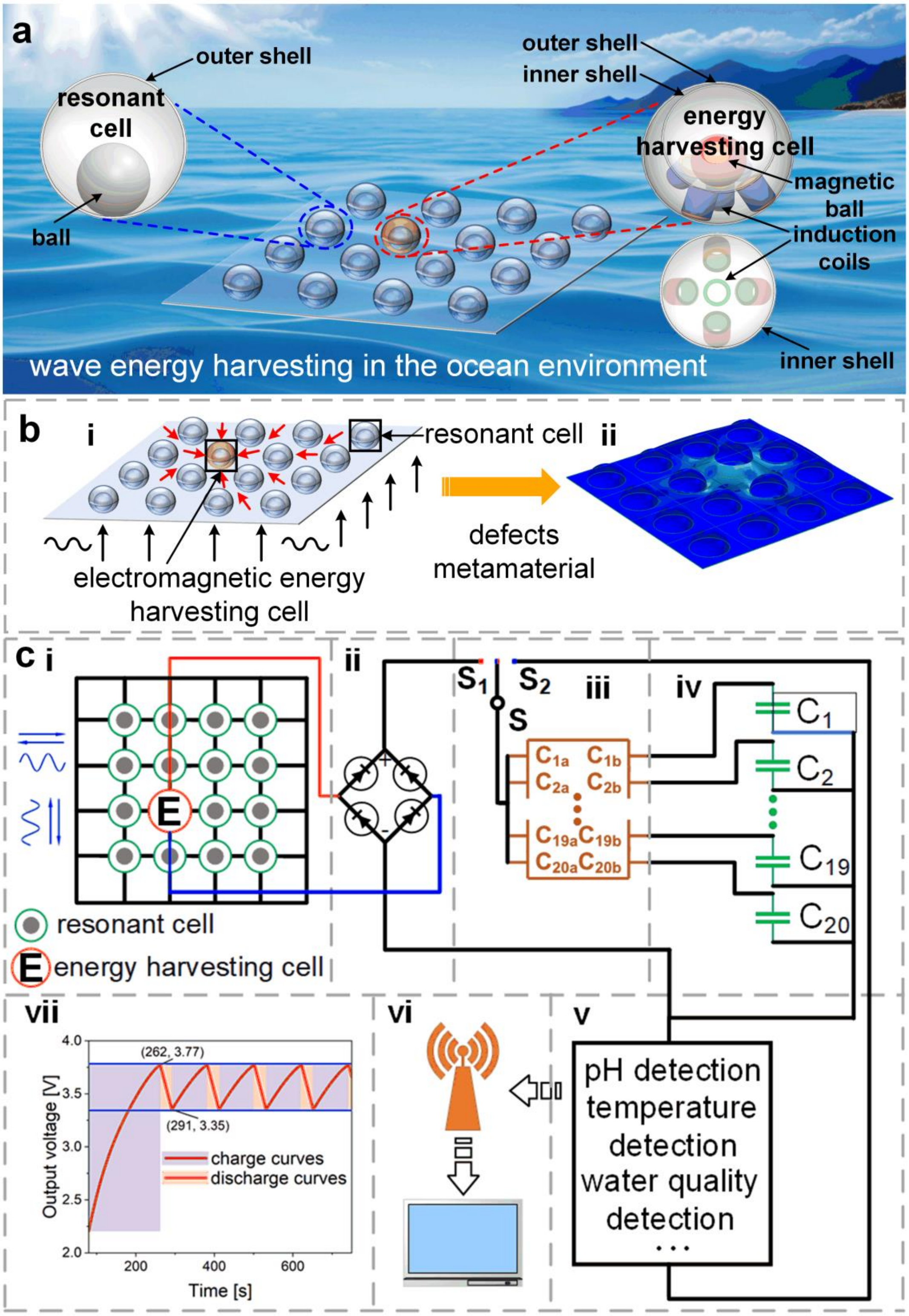

Fig. 1 Design diagram of wave energy harvesting and self-powered health monitoring system in OIoT. a. schematic of a metamaterial energy harvester harvesting wave energy from the ocean

environment. The red dashed circle illustrates the electromagnetic energy harvesting cell and the blue dashed circle illustrates the resonant cell; b: (i) Schematic of the energy concentration phenomenon of the metamaterial with defects under wave excitation; (ii) Simulated displacement clouds of metamaterial plates with point defects when excited by ocean waves, c. schematic design of a self-powered ocean environmental health monitoring system: (i) high-density wave energy harvesting metamaterial panels. The green circle illustrates the resonant cell and the red circle illustrates the energy harvesting cell, (ii) rectifier module (AC→DC); (iii) Series/parallel conversion module for energy storage elements. (S is a single-patch double-throw switch (ADG719-EP) integrated into the circuit to achieve series/parallel conversion of the energy storage element. When S_1 is closed, the capacitors are connected in parallel and the energy storage element is charged; when S_2 is closed, the capacitors are connected in series and the energy storage element is discharged); (iv) energy storage module; (v) environmental condition monitoring module (e.g. pH, temperature, and water quality); (vi) monitored information receiving module; and (vii) charge/discharge curves of the energy storage modules;

(3) The outputs are trivial in the context of water wave energy harvesting and when looking into scaling up the design, more efficient and standard wave generators already exist, so the actual and practical use of such system is unclear rather than powering small electronics which could be powered by a small battery for several years rather than using such complicated mechanism with several units in a relatively large system.

Response: In the process of establishing the ocean IoT, it is impractical to have a standard wave generator for the environmental monitoring sensors. Small batteries may pollute the ocean environment and have limitted discharging capacity, so it is necessary to design efficient energy-harvesting devices for small ocean environment monitoring systems. The ocean environmental health monitoring system proposed in this study consumes relatively little energy and does not require a large wave harvester. The integrated design of energy harvesting and health monitoring enables stable and long-lasting monitoring of the ocean environment.

Changes:

On Page 23

To validate the monitoring effectiveness of the self-powered ocean environment monitoring system, this section conducts field application tests on the self-powered monitoring system. Fig. 5a shows a complete self-powered ocean environment monitoring system, which mainly consists of high-density energy harvesting metamaterials and environment monitoring software. Fig. 5b shows the experimental photographs of the self-powered ocean environment monitoring system in the day-time and night-time segments of the application. The self-powered ocean environment monitoring system was subjected to real-world environmental experiments in two time periods. The wind speed is 4.5m/s during the daytime from 06:00 to 21:00 and 4.2m/s during the nighttime from 21:00 to 06:00.

To clarify the target frequency of the metamaterial energy harvesting device for realizing the energy concentration phenomenon, the real-time wave height monitoring function of the energy harvesting device was used to derive the wave height monitoring data. The real ocean environment excitation has random spectrum featrure as shown in Fig. 5c(i and ii). (the red solid line is the instantaneous wave spectrum at 00:00-00 and the blue dashed line is the instantaneous wave spectrum at 12:00-12:10).The ocean wave frequencies are distributed within 0.1–2.1 Hz but are primarily concentrated in the frequency ranges of 0.5–1 Hz and 1.5–1.9 Hz. Therefore, the energy concentration frequency of the metamaterial energy harvesting device locates at those frequency ranges, resulting in better energy harvesting efficiency. Fig. 5c(iii) shows the spectrum of the output power of the high-density energy harvesting metamaterials, and shows that the output power is maximum near the defect band, with the maximum output power of 21.1 mW and 22.8 mW in the two time periods, respectively. Fig. 5d shows the real-time monitoring of ocean information by the ocean environment health monitoring system, which can prove that the presented self-powered ocean environment monitoring system has good practicability. In the experiment, the wave energy high-density energy harvesting device based on the defective state characteristics of metamaterials was connected to the monitoring device with wires, and the parts were sealed with hot melt adhesive to waterproof the system to ensure the hermeticity of the ocean environmental health detection system.

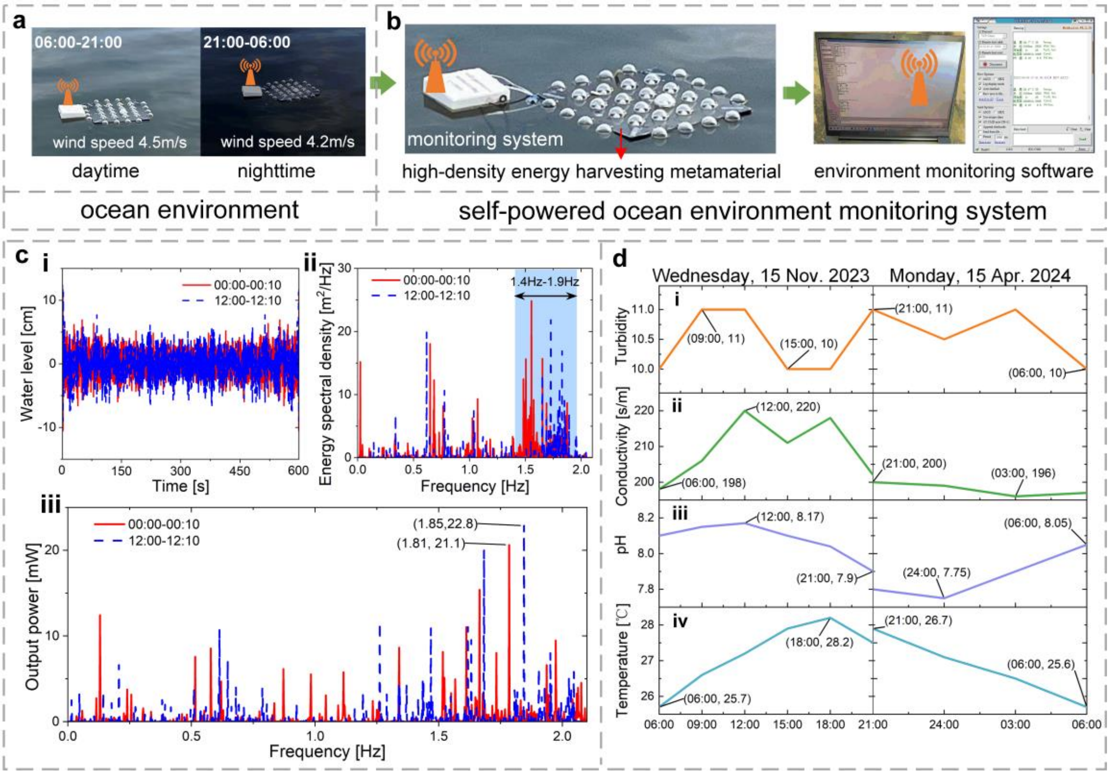

Fig. 5. Self-powered ocean environment monitoring system. a. Self-powered ocean environment monitoring system (High-density energy harvesting metamaterials and environmental monitoring software); b. Schematic diagram of the experiment in the ocean environment: daytime test environment (wind speed of 4.5 m/s) and nighttime test environment (wind speed of 4.2 m/s); c. Experimental results (red solid line: 00:00-00:10; blue dotted line: 12:00-12:10): (i) spectrum of wave levels; (ii) energy spectral density of the wave; (iii) Output power spectra of high-density energy harvesting metamaterials; d. real-time health monitoring results of the ocean environment in one day (24h): (i) turbidity, (ii) conductivity, (iii) pH, and (iv) temperature.

(4) The effect of random motion and random excitation have not been investigated systematically as it may exist in water waves and is important in realizing whether a stable output would be achieved under such condition or not.

Response: Thank you for the constructive comment. To show the performance of the harvester under random motion and ectitaition, an ocean wave environment simulation test platform is built, which can simulate various working conditions in the ocean environment, including multi-directional excitation, harsh wave conditions, and energy harvesting device flip-over state, etc., and the metamaterial energy harvesting device has a superior energy output performance in all the states. Furthermore, the self-powered ocean environmental health monitoring system was tested in an real ocean environment, which has random spectrum featrure. The test results show that the high-density energy harvesting device has a stable output under the random excitation, and the self-powered ocean environmental health monitoring system can operate effectively.

Changes:

On Page 13

As illustrated in Figs. 3a and 3b, the experiments simulated wave excitation in both stable and harsh environments, examining the motion states and energy output voltages of the rolling ball within the energy-harvesting metamaterial device under different wave excitation states. In harsh ocean environments such as typhoons, the acceleration of waves is generally greater than 0.5g[64,65], which is related to many factors such as ocean depth, area, and wave period. The acceleration of waves is used as an index to distinguish stable and harsh ocean wave environments. Table 2 shows the conditions used to simulate different types of ocean wave environments. The experiments revealed that when the water tank's acceleration was less than 0.5g, small stable waves were generated. When the acceleration was 0.5g, large stable waves were generated. When the acceleration was larger than 0.5g, the wave becomes huge. When the acceleration was greater than 2g, the waves in the water tank significantly impacted the metamaterial energy harvesting device, occasionally causing the metamaterial plate to flip over. Thus, in this study, the simulated ocean waves under different excitations are classified as stable waves and harsh waves. When the applied acceleration exceeds 2g, the wave impact on the water tank may cause the metamaterial to break. Consequently, the maximum excitation acceleration is limited to 2g.

Table 2. Conditions of the ocean wave environment simulation experiments

Excitation acceleration[1] [g]	Excitation direction	Metamaterial plate	Simulation of the ocean wave environment
0.1	*x*-direction	no flip	stable
0.5	*x*-direction	no flip	stable
1	*x*-direction	no flip	harsh
1.5	*z*-direction	no flip	harsh
1.5	*x*-*y* direction	flip	harsh
2	*z*-direction	flip	harsh

[1] In harsh ocean environments such as typhoons, the acceleration of waves is generally greater than 0.5g[64,65], which is related to many factors such as ocean depth, area, and wave period. The acceleration of waves is used as an index to distinguish stable and harsh ocean wave environments.

On Page 23

To clarify the target frequency of the metamaterial energy harvesting device for realizing the energy concentration phenomenon, the real-time wave height monitoring function of the energy harvesting device was used to derive the wave height monitoring data. The real ocean environment excitation has random spectrum featrure as shown in Fig. 5c(i and ii) (the red solid line is the instantaneous wave spectrum at 00:00-00 and the blue dashed line is the instantaneous wave spectrum at 12:00-12:10).The ocean wave frequencies are distributed within 0.1–2.1 Hz but are primarily concentrated in the frequency ranges of 0.5–1 Hz and 1.5–1.9 Hz. Therefore, the energy concentration frequency of the metamaterial energy harvesting device locates at those frequency ranges, resulting in better energy harvesting efficiency. Fig. 5c(iii) shows the spectrum of the output power of the high-density energy harvesting metamaterials, and shows that the output power is maximum near the defect band, with the maximum output power of 21.1 mW and 22.8 mW in the two time periods, respectively.

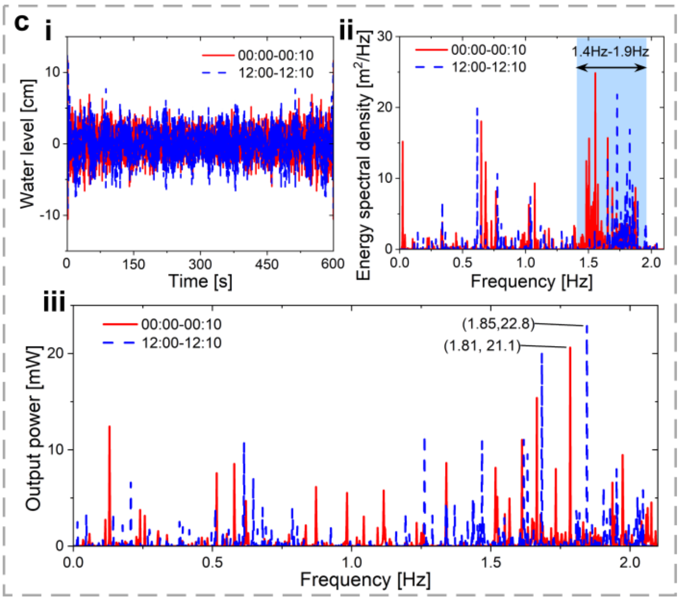

Fig. 5. Self-powered ocean environment monitoring system. c. Experimental results (red solid line: 00:00-00:10; blue dotted line: 12:00-12:10): (i) spectrum of wave levels; (ii) energy spectral density of the wave; (iii) Output power spectra of high-density energy harvesting metamaterials

Once again, the authors thank all the reviewers for their careful reviews of this manuscript with all detailed and constructive suggestions, which have greatly helped to improve the quality of this manuscrip

REVIEWERS' COMMENTS

Reviewer #1 (Remarks to the Author):

The authors have addressed all my comments and answered all of the raised concerns, adequately.
I recommend this paper for publication.

Reviewer #2 (Remarks to the Author):

Authors have revised the paper per the comments, and it is now acceptable.